V2I Infrastructure Placement and Safety Implications of CAVs in an interconnected Network

SAFETY RESEARCH USING SIMULATION

UNIVERSITY TRANSPORTATION CENTER

Zhaomiao Guo, PhD
Assistant Professor
Department of Civil, Environmental and Construction Engineering
University of Central Florida

Fatima Afifah, MSc
PhD Student
Department of Civil, Environmental and Construction Engineering
University of Central Florida

V2I Infrastructure Placement and Safety Implications of CAVs in an Interconnected Network

Zhaomiao Guo, PhD
Assistant Professor
Department of Civil, Environmental and Construction Engineering
University of Central Florida
https://orcid.org/0000-0002-1665-5437

Fatima Afifah, MSc
PhD Student
Department of Civil, Environmental and Construction Engineering
University of Central Florida
https://orcid.org/0000-0001-8434-8124

A Report on Research Sponsored by

SAFER-SIM University Transportation Center

Federal Grant No: 69A3551747131

May 2021

DISCLAIMER

The contents of this report reflect the views of the authors, who are responsible for the facts and the accuracy of the information presented herein. This document is disseminated in the interest of information exchange. The report is funded, partially or entirely, by a grant from the U.S. Department of Transportation's University Transportation Centers Program. However, the U.S. Government assumes no liability for the contents or use thereof.

TECHNICAL REPORT DOCUMENTATION PAGE

1. Report No. UCF-1-Y3	2. Government Accession No.	3. Recipient's Catalog No.
4. Title and Subtitle IV2I Infrastructure Placement and Safety Implications of CAVs in an Interconnected Network		**5. Report Date** May 1, 2021 **6. Performing Organization Code** Enter any/all unique numbers assigned to the performing organization, if applicable.
7. Author(s) Zhaomiao Guo, Ph.D. https://orcid.org/0000-0002-1665-5437 Fatima Afifah, MSc https://orcid.org/0000-0001-8434-8124		**8. Performing Organization Report No.** Enter any/all unique alphanumeric report numbers assigned by the performing organization, if applicable.
9. Performing Organization Name and Address University of Central Florida Department of Civil, Environmental, and Construction Engineering 12800 Pegasus Drive, Suite 211 Orlando, Florida 32816-2450		**10. Work Unit No.** **11. Contract or Grant No.** Safety Research Using Simulation (SAFER-SIM) University Transportation Center (Federal Grant #: 69A3551747131)
12. Sponsoring Agency Name and Address Safety Research Using Simulation University Transportation Center Office of the Secretary of Transportation (OST) U.S. Department of Transportation (US DOT)		**13. Type of Report and Period Covered** Final Research Report (August 2020 – January 2022) **14. Sponsoring Agency Code**

15. Supplementary Notes

This project was funded by Safety Research Using Simulation (SAFER-SIM) University Transportation Center, a grant from the U.S. Department of Transportation – Office of the Assistant Secretary for Research and Technology, University Transportation Centers Program.

16. Abstract

With communication and computational capabilities of connected and automated vehicles (CAVs) evolving rapidly overtime, CAVs can receive and process large amount of data in real-time to dynamically adjust their travel states (e.g., speed, lanes, and/or travel paths). Because of these advanced features, CAVs have great potential to improve the mobility and safety of transportation systems. Existing research has been conducted to leverage infor- mation sharing through vehicle-to-vehicle (V2V) and vehicle-to-infrastructure (V2I) technolo- gies to mitigate intersections and road segments safety risks. However, since transporta- tion is an interconnected network, local traffic adjustments (such as flow or speed changes) could lead to broader impacts by traffic diversion. Therefore, research is urgently needed to investigate the safety implications from a system perspective with these advanced technolo- gies. In this project, we focus on the impacts of information-sharing locations of V2I devices on the system-level safety implications considering adaptive decision-making of CAVs with information updates through V2I communication nodes. We propose a novel transportation network equilibrium model to consider the adaptive decision making of CAVs responding to mobility information updates along their travel paths. Microscopic simulation is conducted to estimate key parameters for network equilibrium model, including surrogate safety measure- ments (e.g., time-to-collision (TTC)), collision risk functions, and link performance functions. Different V2I information sharing strategies are evaluated and compared to understand the impact of information sharing locations on transportation network safety with CAVs using both a four-node test network and Orlando transportation network. We found that: (1) more information shared is not always better for network safety; (2) information sharing at differ- ent locations could dramatically impact the network safety risk; (3) information sharing will influence the rerouting decisions and the collision risk for those links that vehicles reroute to after receiving information updates will determine the network safety. The specific im- pacts of information sharing locations will depend on specific settings of the network but the proposed methodology provides a general way to quantify the impacts for different network settings.

17. Key Words	18. Distribution Statement		
Highways; Planning and Forecasting; Safety and Human Factors; Vehicles and Equipment	No restrictions. This document is available through the SAFER-SIM website, as well as the National Transportation Library		
19. Security Classif. (of this report)	**20. Security Classif. (of this page)**	**21. No. of Pages**	**22. Price**
Unclassified	Unclassified	74	

Form DOT F 1700.7 (8-72) Reproduction of completed page authorized

Table of Contents

List of Figures

List of Tables

Abstract

With communication and computational capabilities of connected and automated vehicles (CAVs) evolving rapidly overtime, CAVs can receive and process large amount of data in real-time to dynamically adjust their travel states (e.g., speed, lanes, and/or travel paths). Because of these advanced features, CAVs have great potential to improve the mobility and safety of transportation systems. Existing research has been conducted to leverage information sharing through vehicle-to-vehicle (V2V) and vehicle-to-infrastructure (V2I) technologies to mitigate intersections and road segments safety risks. However, since transportation is an interconnected network, local traffic adjustments (such as flow or speed changes) could lead to broader impacts by traffic diversion. Therefore, research is urgently needed to investigate the safety implications from a system perspective with these advanced technologies. In this project, we focus on the impacts of information-sharing locations of V2I devices on the system-level safety implications considering adaptive decision-making of CAVs with information updates through V2I communication nodes. We propose a novel transportation network equilibrium model to consider the adaptive decision making of CAVs responding to mobility information updates along their travel paths. Microscopic simulation is conducted to estimate key parameters for network equilibrium model, including surrogate safety measurements (e.g., time-to-collision (TTC)), collision risk functions, and link performance functions. Different V2I information sharing strategies are evaluated and compared to understand the impact of information sharing locations on transportation network safety with CAVs using both a four-node test network and Orlando transportation network. We found that: (1) more information shared is not always better for network safety; (2) information sharing at different locations could dramatically impact the network safety risk; (3) information sharing will influence the rerouting decisions and the collision risk for those links that vehicles reroute to after receiving information updates will determine the network safety. The specific impacts of information sharing locations will depend on specific settings of the network but the proposed methodology provides a general way to quantify the impacts for different network settings.

1 Introduction

The market penetration of connected and automated vehicles (CAVs) is projected to reach approximately 8 million by 2025 [1]. Due to their potential significance from both business and societal perspectives, tech companies have actively developed CAV-related technologies over the past decade. For example, Waymo, which was previously known as the "Google Self-Driving Car" project, has recently exhibited fully driverless capabilities over a large area in Arizona [2]. Vehicles, such as Tesla Model X/S/3, are equipped with advanced driver assistance systems (ADASs) [1], that assist the control of steering, lane changing, acceleration, and braking, which could be further upgraded in the future to have full self-driving capabilities.

CAVs have great potential to transform our transportation systems with a wide range of mobility and environmental benefits [3]. For example, researchers have used traffic modeling theories (e.g., string stability of car-following (CF), and oscillation of traffic flow) to show the potential of CAVs to reduce congestion and energy consumption [4] or have used microscopic simulation techniques to analyze the impacts of CAVs on reducing large-scale incident-induced congestion [5]. Moreover, researchers have further envisioned the integration of CAVs and mobility-as-a-service (MaaS) to pave the way toward a more reliable and sustainable transportation system [6].

The advances of CAV technologies are also capable of improving traffic safety. Over the past decade, research has investigated the safety benefits of CAVs at technology, node, and link levels. For example, [7] comprehensively evaluated twenty major CAV technologies and estimated their crash avoidance effectiveness; [8] shows that intersection crashes have reduced with a higher market penetration of connected vehicles (CVs); [9] shows that CAVs could reduce intersection delay, fuel consumption whilst ensuring safety for non-signalized intersection control; [10] simulates the traffic at a corridor level and find that even a low market penetration of CAVs could reduce traffic conflicts. However, a transportation system is an interconnected network where local node or link traffic state changes may have broader system impacts through traffic diversion. Research addressing the safety implication of CAVs considering an interconnected transportation network is still limited, which hampers

[1] E.g., Tesla Autopilot https://www.tesla.com/autopilot

the thorough analysis of CAVs' safety impacts on the transportation system. This is the main motivation of this study.

The benefits of CAVs can be amplified by harnessing the power of information in the surrounding environment. With the development of advanced sensing and communication technologies, such as accident detection, 5G networks, and vehicle-to-X (V2X) communication, CAVs are exposed to data at an ever growing scale and intensity. One of the key data sources for CAVs is vehicle-to-infrastructure (V2I) technology. V2I is typically bi-directional, which collects and processes vehicle-generated traffic data and wirelessly share information back with vehicles nearby to inform the drivers about safety, mobility, or environment-related conditions. V2I technologies can be integrated with many infrastructure components, including lane markings, road signs, traffic lights, and roadside devices, to communicate information from/to vehicles.

With advanced on-board computational resources, CAVs are able to process a large amount of data in timely manner and dynamically adjust their travel states (e.g., speed, travel lanes, and/or travel paths) based on the information received. Different information sharing strategies, such as when, where, and what to share with which groups of CAVs will significant influence the decision making of individual vehicles, which collectively determine the network performance. While more data have effectively facilitated the decision making of individual vehicles, two critical questions remain insufficiently addressed from a system perspective: (1) whether more information is always better for the safety of transportation system? (2) how to "smartly" provide information over a network to optimize system safety benefits?

The goal of this research is to better understand the impacts of V2I information sharing with CAVs on traffic patterns and traffic safety at a network level. We focus on the location of information sharing and its impacts on the system-level safety considering adaptive decision making of CAVs with information updates. While various types of information can be shared, this study focus on sharing mobility information of specific transportation links with CAVs when they passing by V2I devices. The main contribution of this study is two-fold. First, we propose a novel and mathematical tractable transportation network modeling framework to consider the adaptive decision making of CAVs with information updates. Sec-

ond, we integrate microsimulation techniques with network modeling to evaluate the impacts of information sharing locations on transportation network safety.

The remaining of this report is organized as follows. Section 2 summarizes literature about safety implications of CAV, network safety, and adaptive decision making with information updates. Section 3 explains the methodology used for this study, which includes traffic network modeling with information updates, parametric estimation using microsimulation techniques and real data, and interconnected network safety analyses. Section 4 analyzes the results using a four-node test network and the Orlando transportation network. Section 5 concludes the report and discusses about possible extensions and policy implications.

2 Literature Review

CAVs and V2I technologies provide tremendous opportunities to improve traffic safety through effective vehicle control and information sharing strategies. In this section, we review relevant literature in the following three aspects: (1) existing safety applications of CAVs, (2) studies on network safety, and (3) adaptive decision making of CAVs with information updates.

2.1 Safety Applications of CAVs

CAVs have to progress through multiple levels of automation before fully automated. The Society of Automotive Engineers (SAE) defines 6 levels from fully manual (Level 0) to fully automated (Level 6) [2] [11]. Extensive studies have been conducted to demonstrate the effectiveness of safety improvement leveraging different levels of CAVs. For example, Rahman et al.[8] explore the intersection and road segment safety impacts of CVs with lower level automation (i.e., automated braking and lane keeping assistance) under V2V and V2I communication technologies for intersection safety; Zheng et al.[12] propose a cooperative lane changing strategy with exclusive lanes for CAVs to improve traffic operation, traffic safety and traffic oscillation; Papadoulis et al. [13] develop a CAV control algorithm and sim-

[2] https://www.synopsys.com/automotive/autonomous-driving-levels.html

ulated in VISSIM for motorway segments safety evaluation; Yue et al. [7] comprehensively evaluate twenty major CAV technologies and estimate their crash avoidance effectiveness; Morando et al.[14], [15] investigate the safety impacts of CAVs for a signalised intersection and/or a roundabout.

Since a large-scale penetration of CAVs are not available on the road, existing research typically leverages traffic microsimulation techniques to estimate the surrogate safety measures (gap time, encroachment Time, post-encroachment time, headway, brake rates, speed variation, time-to-collision, etc.) for safety evaluation purposes [12], [14]–[17]. In addition, mixed traffic with different CAVs market penetration rates (MPRs) has been simulated and investigated [8], [13], [16], [17]. All of the aforementioned studies focus on safety applications of CAVs at intersections and/or road segment levels. However, the transportation system is an interconnected network, where the safety implication of CAVs may have broader impacts over a network through traffic diversion.

2.2 Network Safety

Limited studies have been conducted on the implications of network safety with CAVs. Tajalli et al. [18] propose an optimization-based methodology for coordinated speed optimization for CAVs and traffic light control in an urban street network. A mixed-integer non-linear program is developed to model the tradeoff between maximizing network throughput and minimizing network speed variations in the network. However, the network safety implication of CAVs is not investigated. Hasibur and Abdel-Aty [19] are among the first to investigate the mobility and safety impact of CAVs at a network level with both V2V and V2I technologies to communicate with surrounding vehicles and traffic signal using a microsimulation approach. However, information sharing strategies and locations are considered as exogenous, whose impacts on network safety are not investigated.

Another stream of literature aims to understand and predict network safety using different statistical models [20]–[24]. For example, Wang et al. [20] develop Bayesian Conditional Autoregressive (CAR) models to evaluate the safety of various networks as a function of TAZs characteristics and effective road network indices (e.g., closeness centrality, betweenness centrality, and meshedness coefficient). Wang et al. [21] propose a Bayesian

hierarchical joint model to describe the relationship between road network risk and macro-level variables such as socioeconomic, trip generation, and traffic density variables. A Bayesian spatially varying coefficients model is developed by Xu et al.[22] to investigate the spatially varying relationship between crash frequencies and related risk factors using a three-year crash dataset from Florida. Other studies have developed a real-time crash prediction model for traffic safety based on real-time traffic data on road segments [25], [26]. This group of literature typically does not consider the adaptive decision making characteristics of CAVs with dynamic information updates. Therefore, they cannot be directly used to evaluate different information sharing strategies and network safety implications of CAVs.

2.3 Adaptive Decision Making with Information Updates

In order to better characterize the network safety impacts of CAVs and different information sharing strategies, adaptive decision making of CAVs with information updates is needed to be studied. Literature on adaptive decision making can be broadly grouped into three categories. The first category focuses on decision making of a single decision maker and treats the interactions of all other stakeholders and infrastructure systems as exogenous parameters. The second and third categories aim to explicitly model the behaviors of stakeholders and their interactions to provide a description of system outcomes using simulation-based and equilibrium-based approaches, respectively.

2.3.1 Single-agent Adaptive Decision Making

The first category includes a large body of transportation literature using dynamic programming (DP) [27] or reinforcement learning (RL) [28] (also known as neuro-dynamic programming [29] or approximate dynamic programming [30]) to facilitate decision making of a vehicle. DP and RL have been widely used in transportation systems, such as intermodal network planning [31], transportation infrastructure management [32], traffic signal control [33], public transit scheduling [34], and dynamic routing [35]. However, both classic DP or RL suffers from problems of scalability, data sparsity, and knowledge transfer [36]. More recently, RL has been extended to deep RL (e.g. Deep Q-network (DQN)), which leverage deep learning [37] techniques to allow agents directly learn from high dimensional dis-

crete/continuous inputs. Deep RL has many successful applications in different domains, especially games [38], [39], robotics [40], business [41], etc. In transportation, it also shows great potential to mitigate curse of dimensionality [42] and transfer learning [43].

While it is natural to extend single-agent DP/RL/DRL to multi-agent settings, this strategy may not be suitable due to theoretical challenges of non-unique learning goals, non-stationarity, various information structures, and scalability issues [44]. Recent theoretical development in Markov potential games and mean field games mainly focus on homogeneous agents[44] and mean field games are only suitable for the case of large populations of small interacting agents. These limitations make them not directly applicable for heterogeneous multi-agent transportation systems.

2.3.2 Simulation-based Dynamic Traffic Assignment with Real-time Information

Studies have investigated the transportation system dynamics in the framework of simulation-based Dynamic Traffic Assignment (DTA) [45]–[51]. Some studies have explicitly considered the impacts of real-time information updates using iterative approaches to account for drivers' experience and learning processes, which may not lead to convergence. For example, [49] proposes a fixed-point formulation for the user equilibrium with real-time information, which was solved by a heuristic method of successive averages. Based on space-time network, [50] proposes an agent-based optimization modeling framework to determine information provision, which can be solved by integrating Lagrangian relaxation-based heuristics and a mesoscopic DTA simulator. Although simulation-based DTA approaches can characterize system dynamics in detail ideally, it may be extremely challenging to calibrate the simulation parameters for a large network. In addition, rigorous mathematical properties (e.g., existence, uniqueness, and convergence) and structural analyses of system interaction may be challenging to achieve [52].

2.3.3 Equilibrium-based Traffic Flow Modeling with Information Updates

Another stream of literature tries to adapt classic traffic equilibrium notions (e.g., Wardrop user equilibrium [53], [54], stochastic user equilibrium (SUE) [55]–[58], and DTA [59]–[62]) to

capture the impacts of information updates and emerging technologies. For example, [63]–[67] propose equilibrium models for emerging transportation technologies, such as electric vehicles, shared mobility, and connected and autonomous vehicles. However, adaptive decision making with respect to evolving information updates is typically ignored. [68], [69] propose equilibrium routing decision (ERD), an extension of SUE at an individual level and in a shorter time frame. However, ERD treats decision making at each time step as independent of each other. [52], [70], [71] study user equilibrium with recourse (UER) in an uncertain transportation network where travelers adjust their travel routes depending on individual real-time information updates. [72] leverages potential function to represent the Markov decision process routing games in the context of ride-sourcing services, where drivers will consider the routing over an entire time horizon with real-time information updates. All of the above-mentioned research models information implicitly in routing policies, which is challenging for further information design and analyses. In addition, the number of routing policies grows exponentially with both uncertain scenarios and paths, which brings significant challenges for real-world applications. To mitigate these issues, we propose a novel and scalable equilibrium-based network model based on the concept of non-anticipitivity in stochastic programming [73] to characterize the traffic patterns considering the adaptive decision making with information updates.

3 Methodology

The proposed research is to investigate the safety implications of CAVs and V2I technologies considering network interconnection. The proposed methodology include three key modules: *network modeling*, *parametric estimation*, and *safety assessment*, which are illustrated in Figure 3.1. *Network modeling* module takes the output from *parametric estimation* and *safety assessment* modules, such as link performance function and safety risk, to model the traffic patterns with en-route information updates. *Parametric estimation* module estimate parameters in link performance functions and link collision risk functions based microscopic simulation techniques and real-world data for the network modeling and safety assessment purposes. *Network Safety assessment* module utilizes safety surrogate measures generated from *parametric estimation* module and traffic patterns information from

network modeling module to evaluate the safety risks at a network level. These three modules are explained in detail as follows.

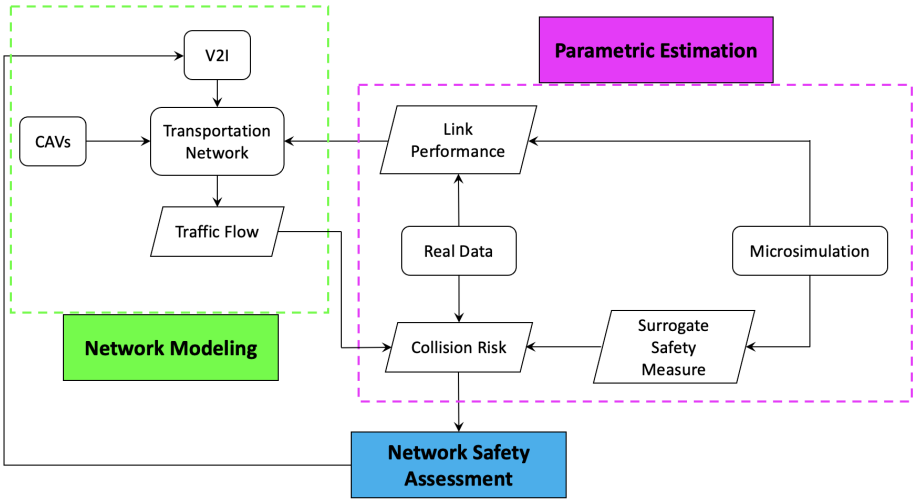

Figure 3.1: Methodology Overview

3.1 Network Modeling

We use network modeling techniques to capture the interdependence between traffic flow at different links and formulate the dynamic decision makings of CAVs when they pass by V2I infrastructure and receive information updates. The information provided by each V2I infrastructure could include travel time, traffic accident/incidents, weather, travel cost, recommended speed, etc. These information are helpful with CAVs since their enhanced data processing capability. The information sensed and communicated with CAVs can be generalized into two categories: link travel time and link collision risk, which correspond to travel efficiency and safety. Notice that in a stochastic environment, these parameters could be communicated with CAVs as random distributions, of which the variance could be used as a measurement for travel reliability. To keep a clear focus, in this study, we assume that CAVs will make routing decisions based on the expected travel time given the information they received. Therefore, network modeling module requires input of stochastic link performance function to allow CAVs to make inform decisions.

Depends on the deployment of V2I devices over network and the travel paths of CAVs, information may be shared with different CAVs at different locations. Similar to classic traffic

assignment, the link travel time and the route choices of all CAVs are coupled. To describe the traffic flow pattern given information updates, we propose a novel formulation of traffic assignment with adaptive routing decision making. In this subsection, we will start with a brief introduction on classic deterministic and stochastic user equilibrium models. Then, we we discuss how to generalize the classic user equilibrium models to reflect the adaptive decision making with information updates.

3.1.1 Classic Traffic Assignment Models

We denote a transportation network as $\mathcal{G} = (\mathcal{N}, \mathcal{A})$, where $\mathcal{N}$ is the node set (indexed by n) and $\mathcal{A}$ is the set of links (indexed by a). Furthermore, we define the OD set $\mathcal{C} \doteq \mathcal{R} \times \mathcal{S}$ (indexed by rs), where $\mathcal{R}, \mathcal{S} \subseteq \mathcal{N}$ are sets of origin and destination nodes. The route (path) set for connecting an OD pair rs ($\in \mathcal{C}$) is denoted as $\mathcal{P}_{rs}$. By Wardrop first principle [53], $\forall p \in \mathcal{P}_{rs}$ with positive path flow (i.e., $x_p > 0$),

$$c_p(\boldsymbol{x}) = \min_{q \in \mathcal{P}_{rs}} c_q(\boldsymbol{x}) \tag{3.1}$$

where $\boldsymbol{x}$ is the path flow vector and $c_p(\cdot)$ is the path travel costs function.

Based on the definition of Wardrop user equilibrium, [74] proposed an equivalent mathematical formalization as (3.2) to facilitate the calculation of link traffic flow $\boldsymbol{v}$ for large-scale transportation networks.

$$\underset{\boldsymbol{v}}{\text{minimize}} \quad \sum_{a \in \mathcal{A}} \int_0^{v_a} t_a(z)\, dz \tag{3.2a}$$

$$\text{subject to} \quad \boldsymbol{v} \in \mathcal{X}_v, \tag{3.2b}$$

where $\mathcal{X}_v$ is the projection into the arc flows space of feasible flow set $\mathcal{X} =: \{(\boldsymbol{v}, \boldsymbol{x})\}$. Notice that $\mathcal{X}_v$ is a polytope and (3.2a) is convex and continuously differentiable [3], model (3.2) is a convex optimization problem and always obtains its global optimum using local gradient information. If the cost function $t_a(\cdot)$ is strictly increasing, then the optimal solution (i.e., link

[3] Because the objective is the integral of a nondecreasing continuous function.

flow pattern) is unique.

However, the definition of Wardrop equilibrium and the corresponding formulation and properties are limited to deterministic case. Stochastic user equilibrium, pioneered by [55], was proposed to model the one-stage routing decision making considering perceived uncertainties of travel time. In other words, classic stochastic user equilibrium assumes travelers to choose a specific route at the beginning of their trips based on perceived uncertain path/link travel time and does not consider the potential information updates during the travel routes.

3.1.2 Adaptive Traffic Assignment Models

Our routing behavior is adaptive to new information provided by V2I about uncertainty of the link travel time. To distinguish from the classic one-stage stochastic user equilibrium notion, we denote our traffic equilibrium as adaptive stochastic user equilibrium (ASUE) in this study. It is important to consider the routing decision in a multi-stage stochastic setting because both large amount of data and computing power are accessible nowadays and the future of transportation may rely on “smart” vehicle technologies, which take advantage of these resources to make sophisticated dynamic routing decisions based on real-time information. Studying this problem may be helpful to answer some critical questions. For example, whether more information is better for the traffic system or not? How to effectively share the information with drivers?

In this study, we focus on a simpler setting, denoted as two-stage ASUE, where only one universal information will be provided at some specific nodes, denoted as information nodes. In other words, we restrict ourselves to the case that all the information nodes will provide the same information on system uncertainties ξ, so that for the first time a driver passing through node $n \in \mathcal{N}_I$, he/she will receive a specific realization of ξ, which will be taken into account for their future routing decisions. This setting indicates that there are at most two stages, i.e. before/after receiving information, of the decision making for drivers traveling on any paths.

To illustrate how to model two-stage ASUE, we start with a simple four-node network,

as shown in Figure 3.2.

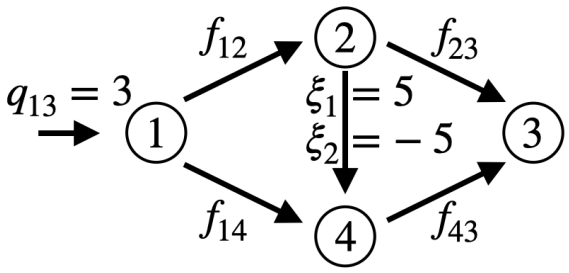

Figure 3.2: Four-node Network with Stochastic Link Cost

In Figure 3.2, there are 3 units of travel demand from node 1 to node 3. The link cost, as a function of link flow f, is shown on each link. The travel cost of link 2-4, denoted as a random variable ξ, is uncertain, which could be influenced by random events, such as traffic accidents or weather events. We assume ξ has two realizations, 5 and -5, with equal probability in this toy example. Node 2 is the only information node that reveals the realization on ξ to the drivers passing by node 2. From node 1 to node 3, there are three paths: $p_1 = \{1, 2, 3\}, p_2 = \{1, 2, 4, 3\}, p_3 = \{1, 4, 3\}$. We assume that all drivers are rational and risk neutral, and have common knowledge on the historic probability distribution of ξ. In the first stage, drivers will decide whether to take link 1-2 or 1-4, considering the historic probability distribution of ξ. If drivers choose link 1-2 in the first stage, they will have an option later to decide whether to go on route 2-4-3 or route 2-3 based on the new information received at node 2. Under this setting, we define the *Two-stage ASUE* in Definition 1.

Definition 1 *(Two-stage ASUE). In two-stage ASUE, the following two conditions hold:*

- *the expected travel costs on all paths used in the first stage are equal, and less than those which would be experienced by a single vehicle on any unused path;*
- *the journey times on all paths used in the second stage are equal, and less than those which would be experienced by a single vehicle on any unused path.*

Notice that the drivers are allowed to switch routes in the second stage. Therefore, "paths selected in the first stage" should bundle all the possible paths that a driver can still choose after they receive uncertain information. In our four-node example (Figure 3.2),

there are two possible "bundled paths" in the first stage: $\mathcal{P}_1^{rs} = \{p_1, p_2\}$ and $\mathcal{P}_2^{rs} = \{p_3\}$. More formally, we define the "bundled paths" as *hyper path*, as shown in Definition 2.

Definition 2 *(hyper path). A hyper path, denoted as $\mathcal{P}_k^{rs}$, is the k^{th} set of paths that connect the same OD pair rs and share the same sequence of links from origin r to the first information node i ($i = s$ if there is no information nodes on a path), such that drivers have not received information before reaching node i.*

Based on Definition 1, we can manually calculated the equilibrium flow, as shown in Table 3.1. From the (expected) costs, as presented in the parenthesis in Table 3.1, we can verify that: (1) (p_1, p_2) and p_3 have the same expected cost [4]; and (2) p_1 has lower second-stage travel cost than p_2 when $\xi = 5$ so that p_1 is selected while p_2 is unused in the second stage for this scenario. Opposite observations hold when $\xi = -5$. The traffic patterns reported in Table 3.1 are dramatically different from the classic user equilibrium solutions, where $x_{p_1} = x_{p_3} = 1.5$, and $x_{p_2} = 0$. The interpretation for this difference is that because V2I is available at node 2, CAVs expect to receive information updates if they travel through $\{(p_1, p_2)\}$ in the first stage. Therefore, more CAVs are willing to choose $\{(p_1, p_2)\}$ compared to $\{p_3\}$ in a two-stage ASUE in contrast to the user equilibrium solutions under Wardrop first principal.

Table 3.1: Equilibrium solutions with risk-neutral adaptive behaviors

Path	Flow		Travel Costs			
	ξ_1	ξ_2	ξ_1	ξ_2	Exp.	Var.
p_1	7/3	0	14/3	-	2.5	9.4
p_2	0	7/3	-	1/3		
p_3	2/3	2/3	4/3	11/3	2.5	2.7

For a general transportation network $\mathcal{G} = (\mathcal{N}, \mathcal{A})$, computing two-stage ASUE manually based on the definition is non-trivial. Inspired by the mathematical formulation of Wardrop equilibrium proposed by [74], we construct a convex optimization problem, whose optimal solutions are consistent with our definition of two-stage ASUE. The convex optimization model that can generate the equilibrium outcome according to Definition 1 is presented in model (3.3).

[4] Note that although the expectation of travel costs of both (p_1, p_2) and p_3 are the same, (p_1, p_2) has higher variance of travel costs compared to p_3. Therefore, for those travelers value reliability of travel costs, more traffic will be shifted from (p_1, p_2) to p_3. This is beyond the focus of this research and will be left for future investigation.

$$\min_{x_p(\boldsymbol{\xi})\geq 0,\ \forall p,\boldsymbol{\xi}} \quad \mathbb{E}_{\boldsymbol{\xi}} \sum_{a\in\mathcal{A}} \int_0^{v_a(\boldsymbol{\xi})} t_a(u,\boldsymbol{\xi})\mathrm{d}u \tag{3.3a}$$

s.t.

$$v_a(\boldsymbol{\xi}) = \sum_{rs\in RS} \sum_{p\in\mathcal{P}^{rs}} \delta_{ap} x_p(\boldsymbol{\xi}),\ \forall a\in\mathcal{A}, \boldsymbol{\xi}\in\boldsymbol{\Xi} \tag{3.3b}$$

$$(\gamma^{rs}(\boldsymbol{\xi})) \qquad \sum_{p\in\mathcal{P}^{rs}} x_p(\boldsymbol{\xi}) = q^{rs},\ \forall rs\in RS, \boldsymbol{\xi}\in\boldsymbol{\Xi} \tag{3.3c}$$

$$(\lambda^{rs}_{a,k}(\boldsymbol{\xi})) \qquad \sum_{p\in\mathcal{P}^{rs}_k} \delta^{+}_{ap} x_p(\boldsymbol{\xi}) = x^{rs}_{a,k},\ \forall rs\in RS, a\in\mathcal{A}, \boldsymbol{\xi}\in\boldsymbol{\Xi} \tag{3.3d}$$

where:

v_a : traffic flow on link a;

$t_a(\cdot,\cdot)$: travel time function of link a;

q^{rs} : travel demand from r to s (model input);

$x_p^{rs}(\boldsymbol{\xi})$: traffic flow on path p that connects r, s at scenario $\boldsymbol{\xi}$;

x_a^{rs} : traffic flow on link a from r to s that haven't received information on $\boldsymbol{\xi}$;

δ_{ap} : link-path incidence scaler, which equals to 1 if link a belongs to path p, and 0 otherwise;

δ^{+}_{ap} : link-path incidence scaler, which equals to 1 if link a belongs to path p and has not passed through any node n $\in \mathcal{N}_I$, and 0 otherwise;

$\mathcal{P}^{rs}_k$: The path set for those paths share the same sequence of links before they receive uncertainties information, with k denote the k^{th} set for rs;

$\boldsymbol{\gamma}, \boldsymbol{\lambda}$: dual variables of corresponding constraints.

The basic idea of model (3.3) is that we first relax path flow x_p and links flow v_a to be scenario dependent, and then enforce non-anticipitivity constrains (3.3d) to guarantee the paths flow is measurable according to the uncertainty set, i.e. the flow on the path segments before receiving information should not depend on $\boldsymbol{\xi}$. Constraint (3.3b) aggregates the path flow to each link for each scenario $\boldsymbol{\xi}$; constraint (3.3c) restricts the summation of paths flow connecting each OD pair should equal to OD demand. The objective function (3.3a) does not carry explicit physical meaning. We construct objective function (3.3a) in this way so that the optimal solutions of optimization problem (**??**) satisfies the two conditions in Definition

1. Therefore, the optimal solutions are two-stage stochastic user equilibrium. This result is stated more formally in Theorem 1.

Theorem 1 *(two-stage ASUE) The traffic flow pattern is under two-stage ASUE if and only if it is the optimal solution to optimization problem (3.3).*

3.2 Parametric Estimation

Network modeling and system safety assessment require link-level information (e.g., traffic link performance function and link crash risk) that may not be directly available from real traffic sensors. In addition, to investigate hypothetical strategies for transportation network planning and information sharing, real-world data are unavailable. To mitigate the impact of data limitation, we use a high-fidelity microsimulation platform, SUMO, to estimate these key parameters for this study. We have chosen SUMO over other microsimulation softwares (VISSIM, AIMSUN, etc.) because of its flexibility to be used with Python programming language and open-source licenses, which maximize the transferability of this study. In this subsection, we will discuss how to estimate the key parameters using microsimulation techniques and real data.

3.2.1 Link Performance Function

Link travel time is typically traffic flow dependent. In classic traffic assignment models [75], link performance functions ($t(v)$) or volume-delay functions are used to express the effect of traffic flow on travel time, which are typically be expressed as free flow travel time (t_0) multiplies by a normalized congestion factor, $f(\frac{v}{c})$, where v/c is the link flow/capacity ratio.

Researchers have used different link performance functions in the past [76]. By far, the Bureau of Public Roads (BPR) function is one of the most widely adopted functions because of its simplicity and convenience to represent congestion behavior and free-flow travel time. The BPR functions are expressed as Equation (3.4).

$$t = t_0[1 + \alpha(\frac{v}{c})^{\beta}] \tag{3.4}$$

where t_0, α, β, and c are parameters that define the shape of the BPR function and needed to be estimated for different types of roadways. The travel time will increase with the ratio of the flow v and the capacity c ($f(\frac{v}{c})$) to represent congestion effects.

In a stochastic environment, parameters t_0, α, c, and β in link performance function (3.4) will be random variables. The link performance function at a specific scenario $\xi \in \Xi$ can be expressed in Equation (3.5).

$$t_\xi = t_{0,\xi}[1 + \alpha_\xi(\frac{v_\xi}{c_\xi})^{\beta_\xi}] \tag{3.5}$$

where $\boldsymbol{\xi} = \{t_{0,\xi}, \alpha_\xi, c_\xi, \beta_\xi\}$ are random parameters that are not known to the travelers at the beginning of their trips and could be updated along the CAVs' travel paths if V2I information sharing is available. The information that CAVs receive from V2I infrastructure is assumed to be the probability distribution of these random parameters.

Link travel time t will depend on the uncertain parameters $\boldsymbol{\xi}$ in addition to link flow v. To estimate the parameters $\boldsymbol{\xi}$ for a specific scenario, we use non-linear least squares regression. The input data for the regression model is (t, v), which could be simulated in a microsimulation platform when they are not able to be directly measured from real-world traffic sensors.

3.2.2 Surrogate Safety Measures

Safety is a primary concern among transportation engineers in developing new and innovative transportation facilities. Due to the lack of readily available crash data or a good predictive model of crash risks, a research project [77] sponsored by FHWA investigated the prospects of surrogate safety measures from existing traffic simulation models to evaluate safety at both signalized and unsignalized intersections. Surrogate safety measures have been used in the evaluation of intersection safety [78][79], roundabout safety [80], optimization of traffic signal timing [81] , evaluation of collision risk [82][83], etc. There are many proximal surrogate indicators, such as temporal proximal indicators [84][85], distance based proximal indicators [86][87], deceleration based indicators [88] [89] and indicators

specific to certain vehicle movement issues such as jerks [90]. Without loss of generality, we adopt temporal proximal surrogate indicators to illustrate our proposed the methodology.

Over the years, researchers have developed a few temporal proximal surrogate indicators such as Time-to-Collision (TTC)[91], Crash Index (CI) [85], Headway (H) [92], Time-to-Accident (TA) [93][94], and Post-Encroachment Time (PET) [95][96]. TTC has been a widely accepted indicator for rear-end-collision determination; therefore it has been adopted in this study to analyze link-level safety in a network system. Notice that other surrogate indicators can also be adopted without changing the fundamental modeling and analysis strategies in this study. TTC at any given time t is defined as the time remaining for two vehicles to collide if the collision course and speed difference are maintained [91]. The mathematical expression for TTC is shown in Equation (3.6). This formulation is consistent with [84], [97].

$$TTC_i = \begin{cases} \dfrac{X_i(t) - X_{i-1}(t) - l_i}{\dot{X}_i(t) - \dot{X}_{i-1}(t)}, & \text{if} \quad \dot{X}_i(t) > \dot{X}_{i-1}(t) \\ \infty, & Otherwise \end{cases} \tag{3.6}$$

where:

$\dot{X}_i$: the speed of the vehicle i

X_i : the rear position of the vehicle i

l_i : the length of vehicle i

$i-1$: the vehicle in front of vehicle i

All the parameters in Equation (3.6) can be directly retrieved at each microsimulation step using the Traffic Control Interface (TraCI) of SUMO software.

3.2.3 Collision Risk Function

There could be multiple ways of calculating collision risk depends on if real collision data is available or not. When real-world collision data is not available, collision risks can be calculated based on the surrogate safety measures, such as TTC defined in Equation (3.6); when crash data is available, collision risk can be measured as the probability of collision

happen under specific traffic conditions. In this section, we will present the methodology to calculate collision risk in different data availability scenarios. The calculated collision risk will be further used to estimate the relationship between collision risk and link traffic flow.

Collision Risk Based on Surrogate Safety Measures When real-world collision data is not available, we model the collision risk as a piecewise function of TTC depends on whether TTC is greater than a predefined threshold $TTC_{\text{Threshold}}$ or not, as shown in Equation (3.7). This approach has also been adopted in [98].

$$CR_n = \begin{cases} TTC_{\text{Threshold}} - TTC_n, & \text{if} \quad TTC_{\text{Threshold}} > TTC_n \\ 0, & \text{Otherwise} \end{cases} \tag{3.7}$$

where:

CR_n : Collision risk of a link at simulation step n

$TTC_{\textbf{Threshold}}$: TTC threshold

TTC_n : TTC of a link at simulation step n

The interpretation of Equation (3.7) is that when the TTC is greater than $TTC_{\text{Threshold}}$, the situation is considered to be relatively safe, and higher TTC will not further reduce the collision risk because the following vehicles already have sufficient time to respond to an emergency if happen; but when TTC is smaller than $TTC_{\text{Threshold}}$, there is a possibility of collision and the collision risk increase with the decrease of TTC. One of the advantages of the collision risk measures as defined in Equation (3.7) is that collision risk is continuous and bounded within [0, $TTC_{\text{Threshold}}$], which can be further normalized to be within [0,1] to represent a probability measurement.

Since collision risk, in this case, is a continuous variable. A linear regression based model can be used to describe the relationship between collision risks and traffic state. This study adopts a similar approach as [99] and uses a polynomial function to describe the relationship between collision risk (CR) and traffic flow (q). The mathematical expression for collision risk in terms of traffic flow is shown in Equation (3.8).

$$CR^{\text{Link}} = \sum_{k=0}^{K} a_k q^n \qquad k = 0, 1, 2, \cdots, K \tag{3.8}$$

where, a_k is the coefficient of k^{th} order term.

To estimate the collision risk, $TTC_{\text{Threshold}}$ should be chosen to distinguish between relatively safe and critical encounters. Generally, TTC lower than the reaction time and perception is considered unsafe [100]. Different studies suggested different TTC values for intersections. Some have suggested a minimum TTC value of 3.5 seconds for the non-supported drivers, and 2.6 seconds for supported drivers [101], whereas others have suggested TTC value of 1 second at an approach of an intersection ([102] [103]) and 3 second ([104]) and 1.6 seconds ([105]) for signalized intersection. Hirst Graham [106] experimented with a collision warning system and concluded that a TTC value of 4 or 5 seconds provides too many false results. The study also added that a TTC of 4 s could be the discriminating value between cases: (1) where drivers unintentionally find themselves in a dangerous situation, (2) where drivers remain in control.

As can be seen from the above discussion, $TTC_{\text{Threshold}}$ varies among studies. Considering the erroneous result that can be caused by a $TTC_{\text{Threshold}}$ greater than 4 seconds, a TTC value equals 3.5 seconds has been chosen to determine the collision risk in this study.

Collision Risk Based on Real Collision Data When real-world collision data is available, we encode the collision risk using a binary variable Y, with 1 indicates collision happens and 0 indicates no collision. Since the Y is an integer variable in this case, we propose a discrete choice-based crash risk model to model the probability of a collision happens p. The discrete choice-based crash risk model is also adopted by [107] and [51], which model crash risk by logistic regression.

The target variable is a binary indicator Y indicating whether collision happens or not with probability p. In other words, Y is a Bernoulli trial and can be expressed as a probability distribution (3.9).

$$Y \sim \text{Bernoulli}(p) \tag{3.9}$$

Discrete choice model is able to estimate the probability p, indicating that with a probability of p collision may happen (i.e., $Y = 1$) and with a probability of $1 - p$ otherwise. The formulation of the logit model is shown in Equation (3.10) for any given link.

$$logit\,(p) = \log\left(\frac{p}{1-p}\right) = \beta_0 + X\beta_1 \tag{3.10}$$

where:

p : the likelihood of collision happens

β_0 : the constant

X : the explanatory variables, such as traffic flow q

β_1 : the coefficients of the explanatory variables

While explanatory variables X can include different variables, in this study, we focus on traffic flow q. Based on this, collision risk for each link is shown in Equation (3.11).

$$CR^{\text{Link}} = p = \frac{e^{\beta_0+\beta_1 q}}{1 + e^{\beta_0+\beta_1 q}} \tag{3.11}$$

3.3 Network Safety Analyses

In order to conduct analysis on the impact of information sharing locations on network safety analysis, we need to mathematically formulate different information sharing strategies and embed them in the ASUE model (3.3), and quantify the network safety measurement. This section focuses on these two aspects.

3.3.1 Representation of Information Sharing Locations

Denote the set of V2I information sharing locations as $\mathcal{I} \in \mathcal{N}$. When CAVs passed by these locations, CAVs will receive information updates for their future routing decision making.

Denote information node indicator variable $y_n, \forall n \in \mathcal{N}$. $y_n = 1$ if V2I infrastructure is

placed at node n; and $y_n = 0$ otherwise. Denote a path is a collection of K links, i.e., $p = \{a_1, a_2, ..., a_K\}$. δ_{ap}^{+} in Model (3.3) can be calculated using Equation (3.12).

$$\delta_{ap}^{+} = \prod_{n \in \mathcal{N}_{ap}} (1 - y_n) \tag{3.12}$$

where $\mathcal{N}_{ap}$ is the node set on path p before reaching to link a.

Using Figure 3.2 as an example, if V2I infrastructure is placed at node 2,

$$y_n = \begin{cases} 1, & \text{if } n = 2 \\ 0, & \text{otherwise.} \end{cases} \tag{3.13}$$

For path $p_2 = \{1, 2, 4, 3\}$ and link $a = \{(4, 3)\}$, we have $\mathcal{N}_{ap} = \{1, 2, 4\}$. Therefore, $\delta_{ap}^{+} = \prod_{n \in \mathcal{N}_{ap}} (1 - y_n) = 0$. In other words, CAVs traveling on path p_2 have received the information when they reach link $\{(4, 3)\}$.

3.3.2 Network Safety Assessment

Given crash risk CR at link level as a function of link traffic flow q (i.e., Equation (3.8) and Equation (3.11)), we can derive the collision risk (CR) for the network as the total risk experienced by all the vehicles in the network. In a stochastic environment, the parameters a_k and β_0/β_1 in Equation (3.8) and Equation (3.11) for any link a will be random variables. We denoted the collision risk for link a at scenario ξ as $CR_{\text{Link},a,\xi}$. Collision risk for the network at a specific scenario $\xi \in \Xi$ can be expressed in Equation (3.14).

$$CR_{\xi}^{\text{Network}} = \sum_{a \in A} CR_{a,\xi}^{\text{Link}} v_{a,\xi} \qquad \forall\, \xi \in \Xi \tag{3.14}$$

where $v_{a,\xi}$ is the link flow at link a in scenario ξ.

In this study, the network safety indicator is measured as the expected network safety risks, as shown in (3.15). We seek to evaluate the impacts of providing information at different locations on the expected network safety risks, CR^{Network}, which can be calculated

in Equation (3.15).

$$CR^{\text{Network}} = \mathbb{E}_{\boldsymbol{\xi}}\{CR_{\xi}^{\text{Network}}\} \tag{3.15}$$

4 Numerical Examples

In this section, we will use a four-node test network and Orlando transportation network to illustrate how to utilize the proposed methodology to analyze the impacts of V2I infrastructure placement on the overall transportation network safety.

4.1 Four-node Test Network

We create a four-node test network corresponding to Figure 3.2 and conduct microsimulation in SUMO (see Figure 4.1) to generate raw data for estimation of link performance functions and collision risk functions. Each link is one-way and have different number of lanes to avoid merging conflicts [5]. The speed limit for each link is set to be 30 mph and the length of each link is one mile. The simulation was conducted using only passenger vehicles with the default vehicle performance configurations in SUMO.

The only traffic demand is from link e_0 to link e_6, which could be assigned to three routes: $p_1 = \{e_0, e_1, e_2, e_6\}$, $p_2 = \{e_0, e_1, e_5, e_4, e_6\}$ and $p_3 = \{e_0, e_3, e_4, e_6\}$. CAVs utilizing p_1 and p_2 are able to make route adjustments at link e_1 if new information is received before node 2. However, if CAVs choose route p_3, they are not able to reroute because only one route is available from e_3.

4.1.1 Fundamental Diagrams

To verify the realisticity of the microsimulation configurations and settings, we first visualize the traffic output data in fundamental diagrams. Figure 4.2 provides the relationship between flow-speed-density for link e_3. The fundamental diagrams for all other links are

[5] e_0, e_6 have three lanes, e_1, e_4 have two lanes, and others have one lane (i.e., e_2, e_3, e_5)

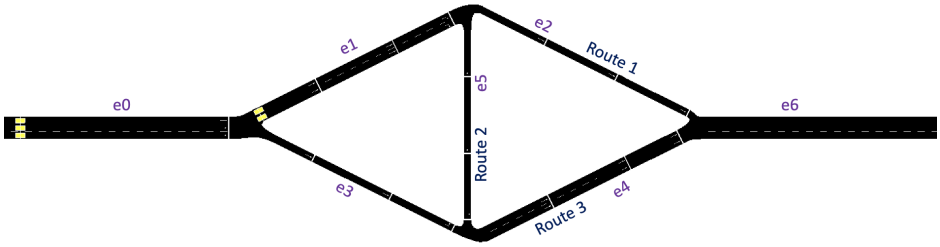

Figure 4.1: Four-node Network in SUMO

provided in Appendix A. Figure 4.2 provides some basic traffic information for link e_3. For example, the free flow speed for the link is around 30 mph (12.5 m/s). The maximum flow of the link is around 1976 veh/hour. These macroscopic traffic statistics are consistent with our simulation settings.

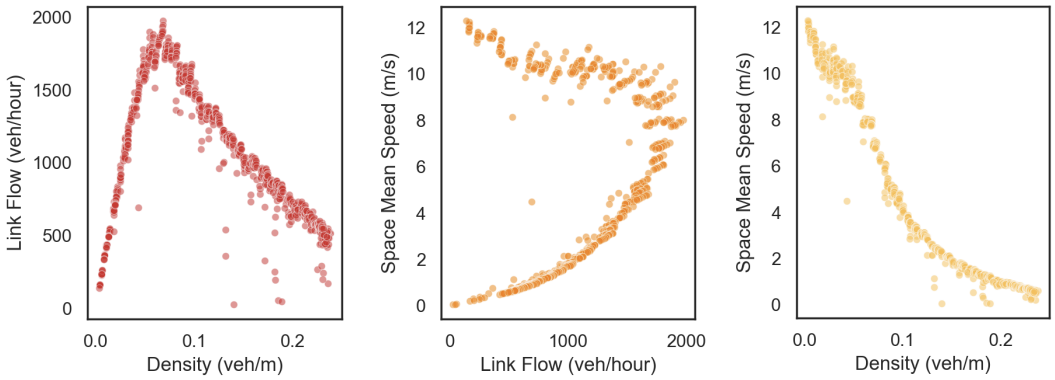

Figure 4.2: Fundamental Diagram of Link e_3

Travel time can be directly calculated using the space-mean speed in Equation (4.1). The link travel time and link flow data will be used to estimate the link performance functions, as discussed in Section 4.1.2.

$$t = \frac{\text{Length of Link}}{\text{Space-mean Speed}} \tag{4.1}$$

4.1.2 Link Performance Function

In this study, we adopt the BPR function form for link performance functions. Notice that using microsimulation, we are not able to capture the relationship between link travel time

and travel demand when travel demand exceeds the link capacity. This is because in microsimulation we only able to measure the actual flow pass links. Therefore, we only use the data when traffic demand is up to the link capacity for the parameter estimation of link performance functions. Using nonlinear regression techniques, we can estimate the parameters in the BPR function, including t_0, α, and β. Equation (4.2) is the resulting mathematical expression for travel time for link e_3 as a function of traffic flow and link capacity ratio.

$$t = 146.843 \left[1 + 2.701 \left(\frac{v}{c}\right)^{3.411}\right] \tag{4.2}$$

Figure 4.3 visualizes the raw data of link traffic flow and travel time as well as the best fitted curve (i.e., Equation (4.2)). The coefficients α and β define the shape of the curve. The fitted curve (Equation (4.2)) rises significantly with the coefficient β (3.411) when the flow is higher at link e_3 to model the congestion effects. The mathematical formulas and visualization of the BPR functions for the other links are provided in Appendix B and Appendix A respectively. The parameters for one-lane and two-lane roads are different. For example, t_0 for two-lane roads is lower than for one-lane roads, although they have the same link length. This is because vehicles on a two-lane road have more flexibility of movement than the vehicles on a one-lane road so that they can travel faster.

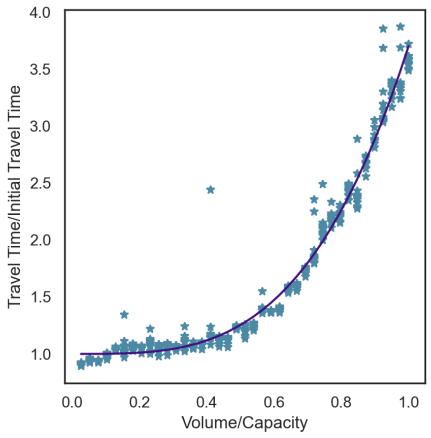

Figure 4.3: Link Performance function of link e_3

4.1.3 Collision Risk Function

As discussed in Section 3.2.3, collision risk at the link level can be modeled using two approaches, i.e., Equation (3.8) and (3.11), depending on whether real collision data are available or not. Since for the four-node test system, we do not have real-world collision data, this section will present the parameters estimation results of the collision risk function using Equation (3.8).

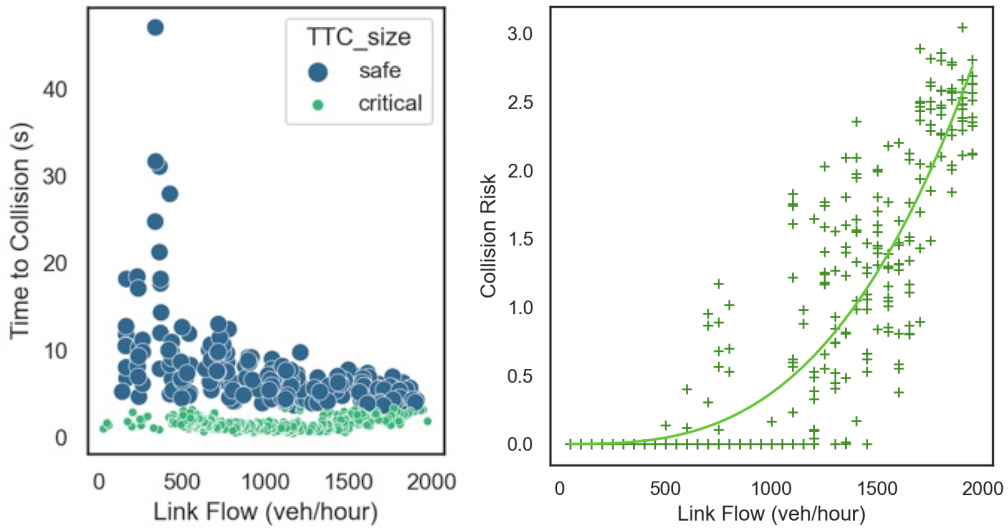

(a) Time-to-Collision vs Flow **(b) Collision Risk vs Flow**

Figure 4.4: Collision Risk vs Flow relationship of Link e_3 using the first approach

As the critical TTC value of 4 seconds or higher gives erroneous results (see Section 3.2.3) and lower TTC provides poor regression coefficients, a $TTC_{\text{Threshold}}$ value of 3.5 seconds has been selected for the model defined by Equation (3.7). Figure 4.4a demonstrates the change of TTC with growing link flow. When the traffic is not congested (blue dots in Figure 4.4a), TTC is higher, providing safer traffic movement. TTC is below 3.5 seconds after traffic flow reaches the link capacity (green dots in Figure 4.4a). The chosen TTC threshold clearly divides the link flow into safe and critical states. Figure 4.4b provides collision risk and flow relationship and it can be best fitted with a third degree polynomial equation with r-squared value of 0.81. The coefficients estimated for Equation (3.8) are shown in Equation (4.3) for link e_3. Collision risk functions for all other links are shown in Appendix B.

$$CR = 6.662e-27+8.306e-28\times Q(k)+6.913e-27\times(Q(k))^2+3.721e-10\times(Q(k))^3 \quad (4.3)$$

4.1.4 Impacts of Information Sharing Locations

Information shared by V2I can influence the traffic patterns, which could lead to an impact on the traffic safety of the whole network. We assume a O-D flow of 15,000 veh/hour and uncertain events (accidents or weather events) could happen on link e_5 to change the link performance function and collision risk function. Different uncertain scenarios can be described by setting different parameters in Equation (3.4) and Equation (3.8). For example, when one lane is blocked due to a traffic accident, the link capacity will be discounted by a certain factor to reflect this scenario. We consider two scenarios for illustration purposes: *Normal Scenario*, where link capacity and safety risk are at their normal levels; and *Incident Scenario*, where the link capacity and safety risk are relatively higher. The uncertain scenarios we consider for this numerical example is shown in Table 4.1.

Table 4.1: Uncertain Scenarios in the Four-node Test Network

Scenario	c of Equation (3.4)	a_3 of Equation (3.8)
Normal	1950	$4.628\text{e}{-10}$
Incident	200	$4.628\text{e}{-9}$

V2I placements at different nodes will influence how each path will respond to the information updates. For example, sharing information at node 4 or node 3 would not change the routing behavior of the road users because even though CAVs receive information updates at nodes 3 or 4, they have only one routing option and cannot make further adjustments to their routes. Information sharing at node 1 indicates that all CAVs will be informed with the information on link e_5 and they can make route choices at the beginning of their trips based on the real transportation network state; information sharing at node 2 will only influence those CAVs choosing path p_1 and p_2, which allow them to choose whether they will reroute or not at node 2. Figure 4.5 shows these three information sharing strategies ((a) *No Information Shared*, (b) *Information Shared at Node 1* and (c) *Information Shared at Node 2*).

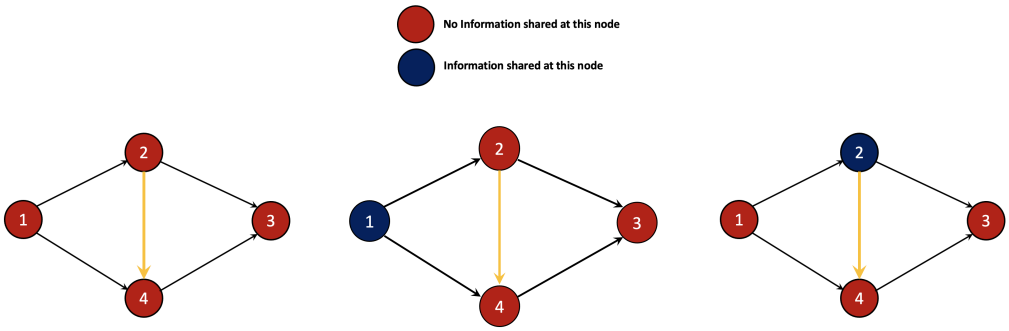

(a) No Information Shared **(b) Info.Shared at Node 1** **(c) Info. Shared at Node 2**

Figure 4.5: Information Sharing in Four-node Network

We have simulate the three infomration sharing strategies, as shown in Figure 4.5. The resulting link flow patterns are shown in Figure 4.6.

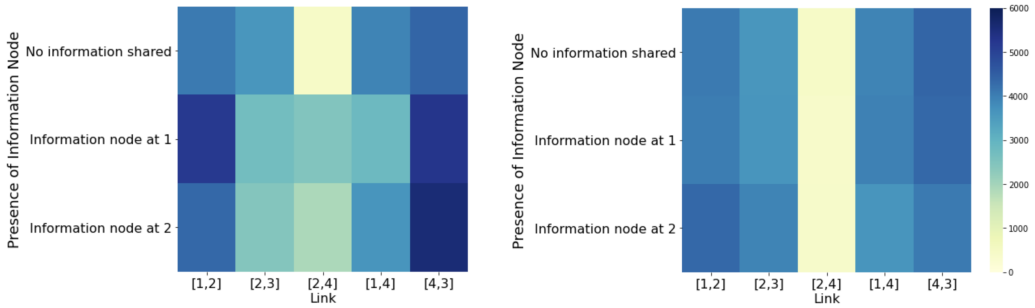

(a) Normal Scenario **(b) Incident Scenario**

Figure 4.6: Link Traffic Flow with Different Information Sharing Strategies

First, in *No information shared* case, the link traffic flow for both scenarios are identical due to the non-anticipativity constraint (3.3d). In other words, people will choose the routes based on their prior knowledge of the network if there is no information updated along their routes. The enforcement of non-anticipativity constraint can also be seen for the case when information shared at node 2, where traffic flow on links 1-2 and 1-4 are identical between both scenarios. This is because on these links, no CAVs pass by information node 2. Therefore, their routing decisions are not measurable to uncertain scenarios.

Second, CAVs are more willing to use the link 1-2 when they are aware of the presence of information nodes at node 1 or node 2, which can be seen in Figure 4.6a and Figure 4.6b. Note that for different information sharing locations, the reasons why more road users traveling on link 1-2 are different. In this particular numerical setting, information shared at node 1 will attract more traffic to go to link 1-2 if the information they received is *Normal*

Scenario. This is because when CAVs know the link 2-4 is in a normal scenario, traveling through link 1-2 will allow them to use two routes p_1 and p_2. However, when the information is shared at node 2, more CAVs travel through link 1-2 because they expect to receive an information update at node 2, where they can make further route adjustments depends on the information received.

Third, once an incident occurs, the traffic patterns will also be sensitive to where CAVs receive the information updates. This can be observed in the cases of *Information Shared at Node 1* and *Information Shared at Node 2* in Figure 4.6b. Since people receive the incident information earlier along the path in *Information Shared at Node 1* case, more road users prefer the link 1-4 over the link 1-2 because path p_2 is not able to be utilized. But in the *Information Shared at Node 2* case, more CAVs will use the link 1-2 since they do not know the incident happen on link 2-4. But as discussed previously, since CAVs can receive information updates immediately before approaching link 2-4, more traffic will use link 2-3 to avoid the incident.

Based on the traffic patterns for different information sharing strategies, we can evaluate the impact of information sharing on the network collision risk, as shown in Figure 4.7. The network has a higher collision risk when there is no information shared at any node. A network is safer when information is shared earlier along the paths comparing between *Information Sharing at Node 1* and *Information Sharing at Node 2*. For this particular network, information shared at Node 1 is equivalent to information being shared at all nodes of that network. This is because anyone passing node 1 will have the same information no matter which route they take to travel thereafter.

However, we note that this case study does not indicate that information sharing is always beneficial to the overall network safety. For example, if link 1-2 has a higher collision risk, more traffic use link 1-2 may lead to higher overall network collision risk even though CAVs can avoid using link 2-4 in the incident scenario. As we discussed previously, since information sharing at node 1 or node 2 will attract more traffic use link 1-2, this will lead to a result that more information sharing will lead to higher overall network collision risk. We will discuss this in more detail using Orlando Transportation Network.

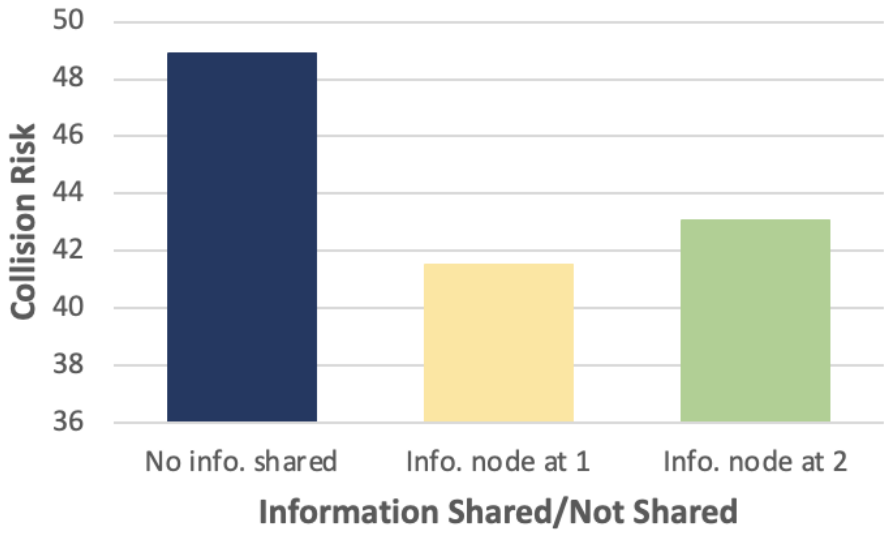

Figure 4.7: Overall Collision Risk

4.2 Orlando Network

In addition to the four-node test network, we test our proposed methodology using Orlando transportation network, as shown in Figure 4.8. The network highlights the traffic between three critical attractions in Orlando metropolitan area, which are Orlando International Airport (Node 17), Universal Studio (Node 11), and Disney world (Node 3). The network covers an area of 78.87 mile^2 (204.27 km^2). This network has a total of 27 two-way links, which comprise both freeways and multi-lanes. The archived traffic data, collected by the Regional Integrated Transportation Information System (RITIS), contains speed data, traffic volume, and occupancy data for each link from multiple sources, including microwave vehicle detectors (MVDs). The average speed and the link flow of each hour at each link were determined using these real traffic data. The crash records during this time period were also collected and aggregated for each hour.

Based on the link traffic and crash data, we are able to estimate the coefficients in Equation (3.11). Appendix C provides the estimated crash risk functions for all the links. In the remainder of this section, we focus on different specific settings of OD traffic demand to evaluate the impact of information sharing on the network collision risk, calculated based on Equation (3.14).

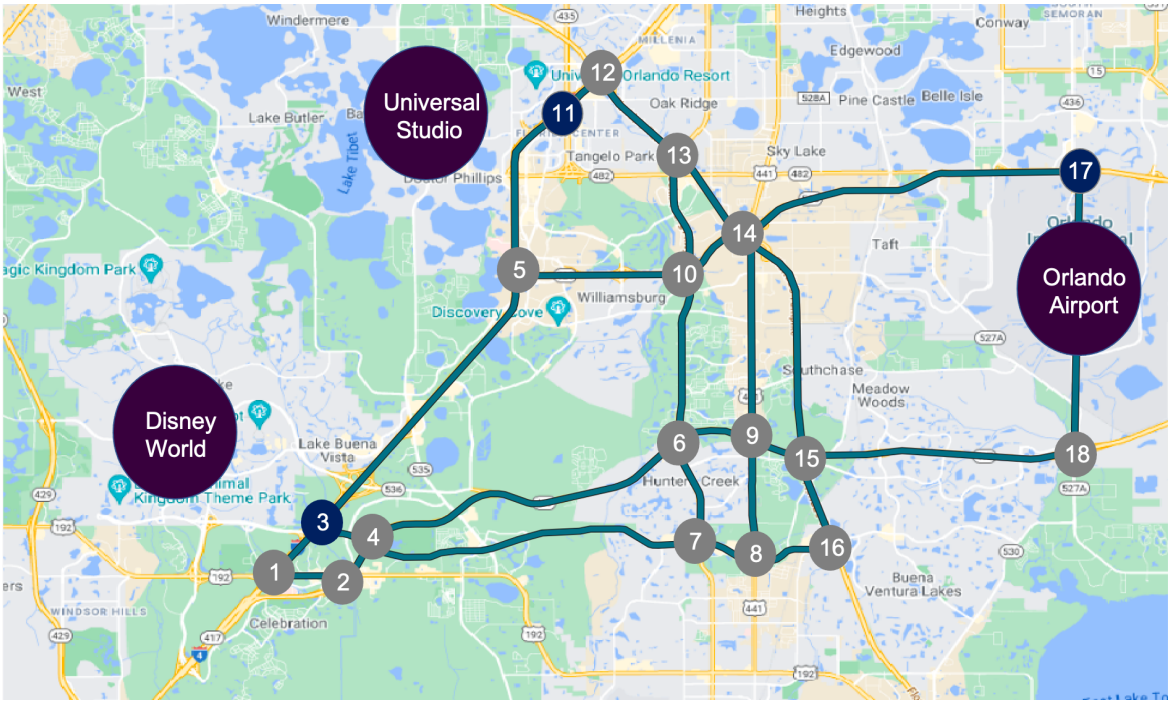

Figure 4.8: Study Area in Orlando

4.2.1 Orlando International Airport to Disney World

The question is if the mobility of a link deteriorates for any reasons, information sharing at which node would lead to the safest network for all travelers. To begin with, we focus on the traffic flow from Orlando International Airport (Node 17) to Disney World (Node 3). The scenario we will investigate is as following: for a given day, the road capacities of links 14-17 and 17-14 could decrease due to traffic incidents, information sharing at which node would make the travel from Airport to Disney World safer. When traffic moves from Airport to Disney World, there is a total of 30 candidate routes (with a maximum of 7 links) (see Table 4.2). The highlighted cells in Table 4.2 show the links of all the routes used. The traffic flow of each route is shown in Figure 4.9.

Figure 4.9 shows traffic in different routes when information is shared at all nodes (*All Share* case) and when information is not shared at all (*No Share* case). There are two scenarios on links 14-17 and 17-14: *normal scenario* and *incident scenario* with equal probability. Note that both of these scenarios are considered when the overall collision risk of the network is evaluated. In *No Share* case, traffic in both scenarios are the same. This is because of the non-anticipativity constraint when uncertainty on the link condition

Table 4.2: All the Possible Routes for Traffic from Airport to Disney World

Route	Links
0	[(17, 14), (14, 9), (9, 6), (6, 4), (4, 2), (2, 1), (1, 3)]
1	[(17, 14), (14, 9), (9, 6), (6, 4), (4, 3)]
2	[(17, 14), (14, 9), (9, 6), (6, 10), (10, 5), (5, 3)]
3	[(17, 14), (14, 9), (9, 6), (6, 7), (7, 4), (4, 3)]
4	[(17, 14), (14, 9), (9, 8), (8, 7), (7, 4), (4, 3)]
5	[(17, 14), (14, 9), (9, 8), (8, 7), (7, 6), (6, 4), (4, 3)]
6	[(17, 14), (14, 10), (10, 5), (5, 3)]
7	[(17, 14), (14, 10), (10, 6), (6, 4), (4, 2), (2, 1), (1, 3)]
8	[(17, 14), (14, 10), (10, 6), (6, 4), (4, 3)]
9	[(17, 14), (14, 10), (10, 6), (6, 7), (7, 4), (4, 3)]
10	[(17, 14), (14, 10), (10, 13), (13, 12), (12, 11), (11, 5), (5, 3)]
11	[(17, 14), (14, 13), (13, 10), (10, 5), (5, 3)]
12	[(17, 14), (14, 13), (13, 10), (10, 6), (6, 4), (4, 3)]
13	[(17, 14), (14, 13), (13, 10), (10, 6), (6, 7), (7, 4), (4, 3)]
14	[(17, 14), (14, 13), (13, 12), (12, 11), (11, 5), (5, 3)]
15	[(17, 14), (14, 15), (15, 9), (9, 6), (6, 4), (4, 3)]
16	[(17, 14), (14, 15), (15, 9), (9, 6), (6, 10), (10, 5), (5, 3)]
17	[(17, 14), (14, 15), (15, 9), (9, 6), (6, 7), (7, 4), (4, 3)]
18	[(17, 14), (14, 15), (15, 9), (9, 8), (8, 7), (7, 4), (4, 3)]
19	[(17, 14), (14, 15), (15, 16), (16, 8), (8, 7), (7, 4), (4, 3)]
20	[(17, 18), (18, 15), (15, 9), (9, 6), (6, 4), (4, 3)]
21	[(17, 18), (18, 15), (15, 9), (9, 6), (6, 10), (10, 5), (5, 3)]
22	[(17, 18), (18, 15), (15, 9), (9, 6), (6, 7), (7, 4), (4, 3)]
23	[(17, 18), (18, 15), (15, 9), (9, 8), (8, 7), (7, 4), (4, 3)]
24	[(17, 18), (18, 15), (15, 9), (9, 14), (14, 10), (10, 5), (5, 3)]
25	[(17, 18), (18, 15), (15, 14), (14, 9), (9, 6), (6, 4), (4, 3)]
26	[(17, 18), (18, 15), (15, 14), (14, 10), (10, 5), (5, 3)]
27	[(17, 18), (18, 15), (15, 14), (14, 10), (10, 6), (6, 4), (4, 3)]
28	[(17, 18), (18, 15), (15, 14), (14, 13), (13, 10), (10, 5), (5, 3)]
29	[(17, 18), (18, 15), (15, 16), (16, 8), (8, 7), (7, 4), (4, 3)]

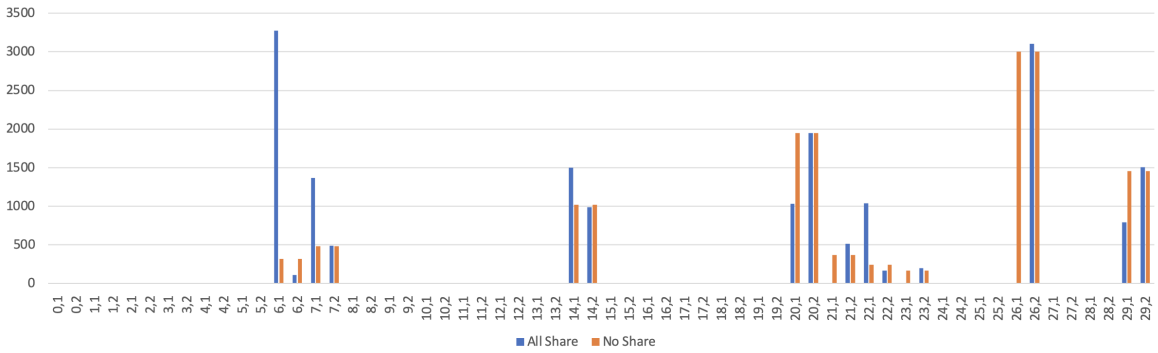

Figure 4.9: Traffic moving from Airport to Disney World using Different Routes

is unknown to the CAVs. To avoid the potential risk of using the link 17-14 when its actual condition is *incident scenario*, most of the travelers will use route 26 and route 20 in *No Share* case. In *All Share* case, since travelers receive information at node 17, travelers can make route choice depends on information received on the real situation of link 17-

14. In *Normal Scenario*, most travelers use route 6, which include link 17-14. However, when in *Incident Scenario*, most people re-route to route 26 from route 6 to avoid utilize the link 17-14 due to its reduced mobility. In this example, *All Share* case is better than *No Share* because in *All Share* people can make routing decisions, learning about the bad road condition, whereas in *No Share* due to lack of information, more people are exposed to risk at link 17-14. The result of this scenario is consistent with the result of the four-node network, i.e., if information is shared at all nodes or at the travel origin, the overall collision risk of the network would be less.

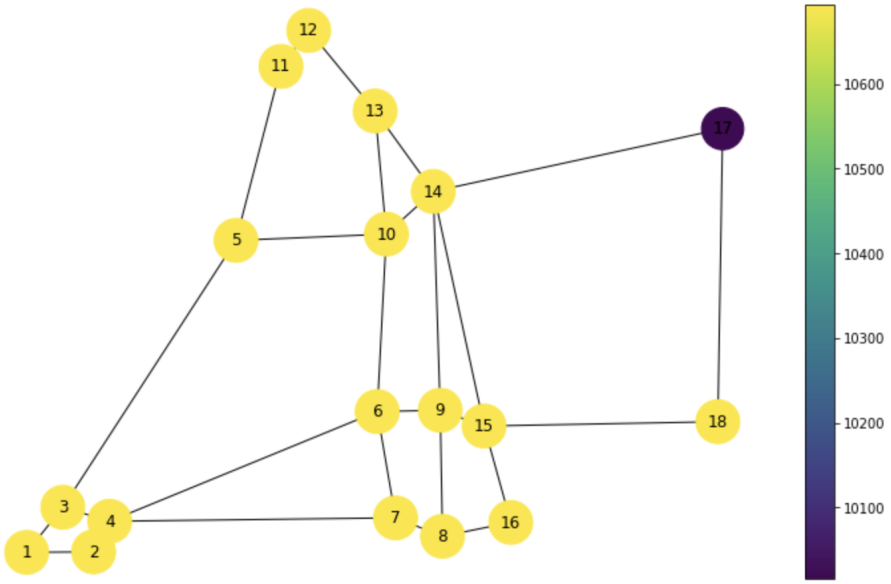

Figure 4.10: Collision Risk for the Traffic Moving from Airport to Disney World

4.2.2 Disney World to Orlando International Airport

Sharing information early at the trip origin lowers the overall risk of the network when the link with uncertain traffic capacity is closer to the origin, as discussed in Section 4.2.1. But it might not be the case if the link with uncertain capacity is further away from the origin. We will focus on the traffic demand from Disney World to Airport in this section. There is a total of 30 routes that people can utilize to travel from Disney World to Airport (Table 4.3). The darkened rows in Table 4.3 show all the links of the routes used (see Figure 4.11).

Identical to Section 4.2.1, we have considered two scenarios: *normal scenario* and *incidence scenario*, where the travel capacities of the links 14-17 and 17-14 decrease. The

Table 4.3: All the Possible Routes for Traffic from Disney World to Airport

Route	Links
0	[(3, 1), (1, 2), (2, 4), (4, 6), (6, 10), (10, 14), (14, 17)]
1	[(3, 1), (1, 2), (2, 4), (4, 6), (6, 9), (9, 14), (14, 17)]
2	[(3, 4), (4, 6), (6, 10), (10, 13), (13, 14), (14, 17)]
3	[(3, 4), (4, 6), (6, 10), (10, 14), (14, 15), (15, 18), (18, 17)]
4	[(3, 4), (4, 6), (6, 10), (10, 14), (14, 17)]
5	[(3, 4), (4, 6), (6, 7), (7, 8), (8, 9), (9, 14), (14, 17)]
6	[(3, 4), (4, 6), (6, 9), (9, 14), (14, 15), (15, 18), (18, 17)]
7	[(3, 4), (4, 6), (6, 9), (9, 14), (14, 17)]
8	[(3, 4), (4, 6), (6, 9), (9, 15), (15, 14), (14, 17)]
9	[(3, 4), (4, 6), (6, 9), (9, 15), (15, 18), (18, 17)]
10	[(3, 4), (4, 7), (7, 6), (6, 10), (10, 13), (13, 14), (14, 17)]
11	[(3, 4), (4, 7), (7, 6), (6, 10), (10, 14), (14, 17)]
12	[(3, 4), (4, 7), (7, 6), (6, 9), (9, 14), (14, 17)]
13	[(3, 4), (4, 7), (7, 6), (6, 9), (9, 15), (15, 14), (14, 17)]
14	[(3, 4), (4, 7), (7, 6), (6, 9), (9, 15), (15, 18), (18, 17)]
15	[(3, 4), (4, 7), (7, 8), (8, 9), (9, 14), (14, 17)]
16	[(3, 4), (4, 7), (7, 8), (8, 9), (9, 15), (15, 14), (14, 17)]
17	[(3, 4), (4, 7), (7, 8), (8, 9), (9, 15), (15, 18), (18, 17)]
18	[(3, 4), (4, 7), (7, 8), (8, 16), (16, 15), (15, 14), (14, 17)]
19	[(3, 4), (4, 7), (7, 8), (8, 16), (16, 15), (15, 18), (18, 17)]
20	[(3, 5), (5, 11), (11, 12), (12, 13), (13, 10), (10, 14), (14, 17)]
21	[(3, 5), (5, 11), (11, 12), (12, 13), (13, 14), (14, 17)]
22	[(3, 5), (5, 10), (10, 6), (6, 9), (9, 14), (14, 17)]
23	[(3, 5), (5, 10), (10, 6), (6, 9), (9, 15), (15, 14), (14, 17)]
24	[(3, 5), (5, 10), (10, 6), (6, 9), (9, 15), (15, 18), (18, 17)]
25	[(3, 5), (5, 10), (10, 13), (13, 14), (14, 15), (15, 18), (18, 17)]
26	[(3, 5), (5, 10), (10, 13), (13, 14), (14, 17)]
27	[(3, 5), (5, 10), (10, 14), (14, 9), (9, 15), (15, 18), (18, 17)]
28	[(3, 5), (5, 10), (10, 14), (14, 15), (15, 18), (18, 17)]
29	[(3, 5), (5, 10), (10, 14), (14, 17)]

path flow in both *normal scenario* and *incidence scenario* when information is either shared at different nodes or not shared at all are illustrated in Figure 4.11. A significant amount of traffic prefers to travel to the information nodes to receive information updates so that they can make informed routing decisions afterwards. For instance, when information is shared at *Node 13*, around 4,000 vehicles out of 8,610 vehicles travel in route 26 in *normal scenario* and re-route to route 25 in the *incidence scenario*. Both routes 25 and 26 pass by node 13.

Figure 4.12 shows the network collision risk using historical crash data for all the links. We can see that the network is safest when information is shared at node 13 and travelers are exposed to higher collision risk when information is shared at node 4. The overall collision risk is evaluated using Equation (3.14) with the inputs - traffic pattern and collision risk of each link.

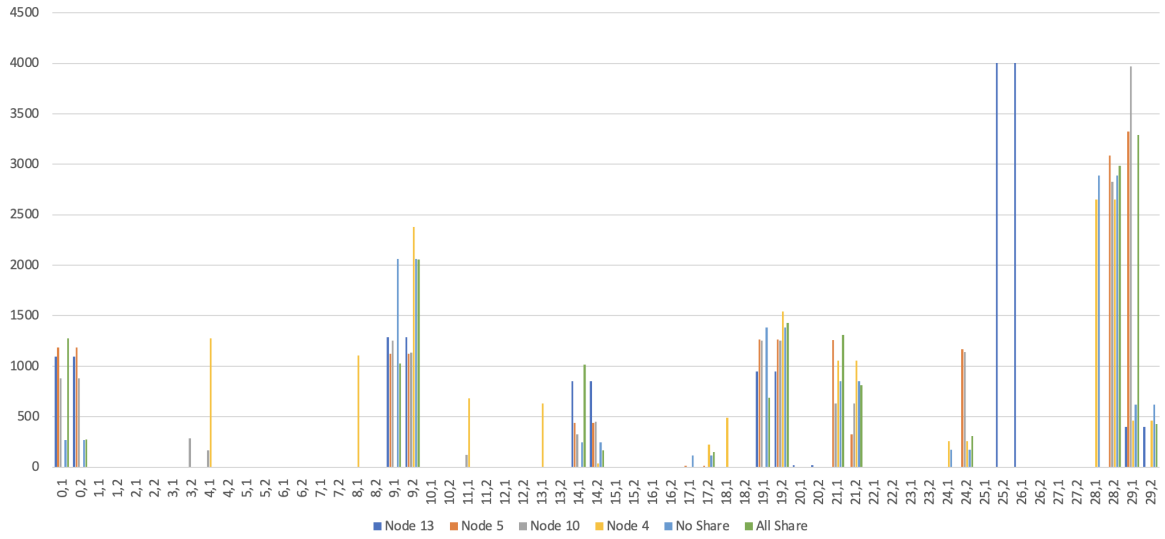

Figure 4.11: Traffic moving from Disney World to Airport using Different Routes

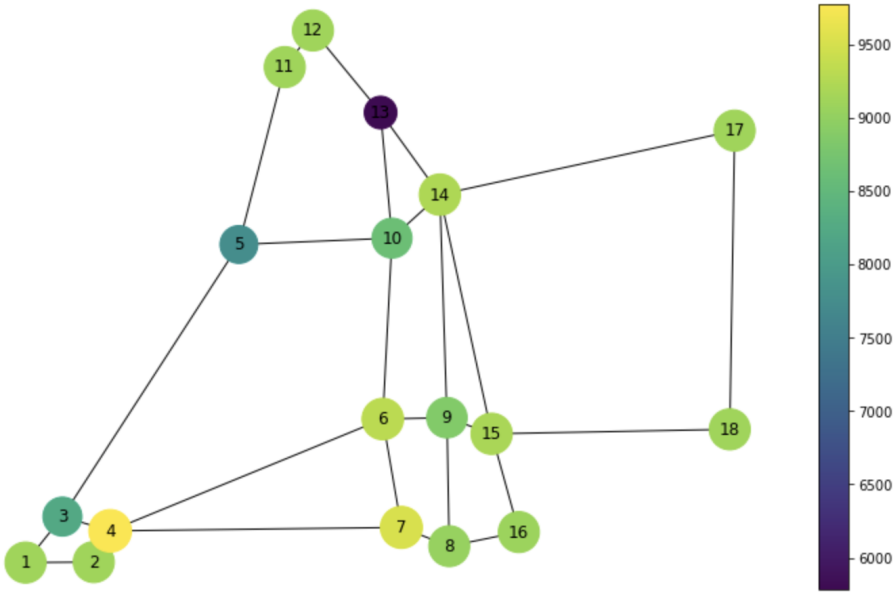

Figure 4.12: Collision Risk for the Traffic Moving from Disney World to Airport

4.2.3 Six OD Pairs

So far, V2I infrastructure placement and its network safety implication have been investigated with one origin and one destination. This subsection will investigate how information sharing locations impact network collision risk when there are multiple origins and destinations considered, i.e., vehicles would enter and leave the network using Airport (Node 17), Universal Studio (Node 11), and Disney World (Node 3). Figure 4.14 shows the impact of information sharing at each node on the network collision risks. Figure 4.13 shows all

routes used when information is shared at all nodes (*All Share*), *Node 17*, *Node 3*, *Node 4*, and *Node 14* for both uncertain scenarios, as defined in Section 4.2.1. There are a total of 114 routes (see Table C.1) when there are six OD pairs. The highlighted cells show all the routes used (see Figure 4.13).

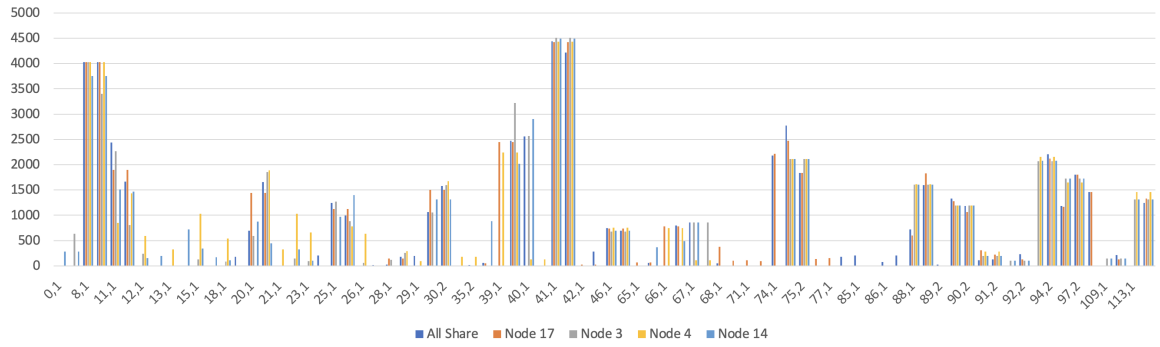

Figure 4.13: All the Traffic from 6 Origins and Destinations using Different Routes

It can be seen that, a significant amount of traffic travels to the information nodes to stay aware of any uncertain events (Figure 4.13). After receiving information most traffic re-route to avoid the link 14-17 when link capacity reduced.

Sharing information at all nodes provides the safest network for this particular setting. When only one information node is allowed, according to Figure 4.14, information sharing at node 6 would make the network safer than information shared at any other nodes. This could be because information sharing at node 6 can benefit the rerouting decisions of more traffic since node 6 lies at a relative centric location of the graph. Information sharing at nodes 1, 2, 4, 7, 8, and 16 may worsen the expected network collision risks due to attracting traffic to take longer detours to these information nodes in order to receive information updates.

5 Discussion

In this study, we investigate the impact of V2I infrastructure placement on transportation network safety. We propose a transportation network modeling framework to model the adaptive routing behavior of CAVs given information updates at different information sharing locations. To estimate the key parameters to support the network modeling and system

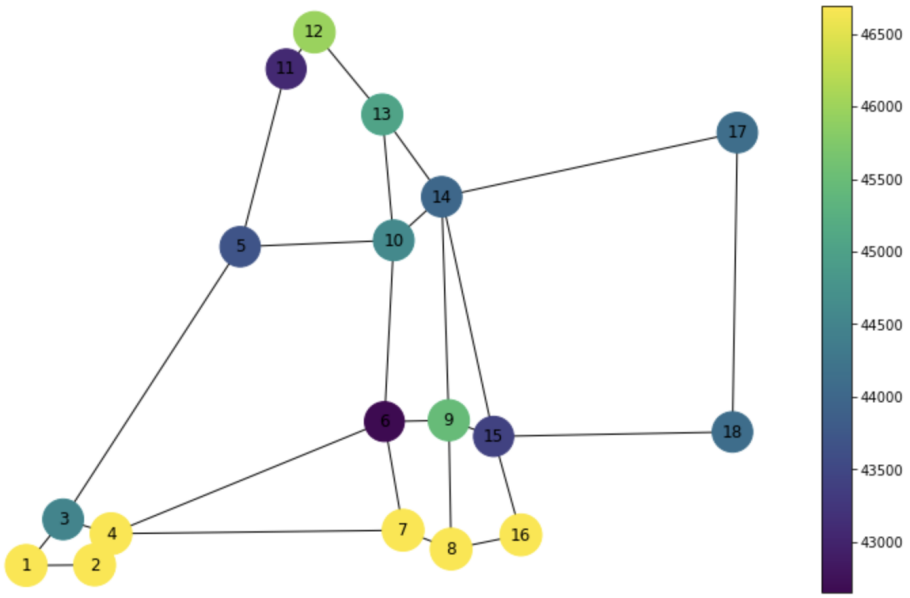

Figure 4.14: Collision Risk for All the Traffic from 6 Origins and Destinations

safety analyses, we conduct parametric estimation based on microsimulation techniques and real-world data. The proposed methodology allows us to identify the optimal location to share information with CAVs that helps to promote the safety of the whole network.

We implement the proposed methodology using both a four-node test network and Orlando transportation network. We found that: (1) more information shared is not always better for network safety; (2) information sharing at different locations could dramatically impact the network safety risk; (3) information sharing will influence the rerouting decisions. The collision risk for those links that vehicles reroute to after receiving information updates will determine the network safety; (4) the specific impacts of information sharing locations will depend on specific settings of the network but the proposed methodology provides a general way to quantify the impacts for different network settings.

This research can be extended in several directions. First, this study aims to provide a general methodology to study the impacts of information sharing locations on network safety. More numerical examples and calibration are needed to fully understand the impacts. Second, we assume there is only one universal information in the network. How to extend the proposed methodology to consider heterogeneous information sharing remains to be solved. But extending the proposed ASUE from two-stage to multi-stage will not change the overall modeling strategies. Third, in addition to information sharing loca-

tions, other aspects of information sharing strategies can be investigated, such as what information to share, to which group of CAVs to share information. Fourth, this study only considers routing decisions based on mobility information. Other routing objectives can be considered, such as reliability, safety, and sustainability. Fifth, given an increasing concerns of cyber security, investigating how the transportation network safety will be influenced with erroneous information is a valuable next step.

6 Acknowledgement

This research was supported by Safety Research Using Simulation (SAFER-SIM), University Transportation Center. We would like to thank Dr. Mohamed Abdel-Aty for his suggestions and data provision to this research. In addition, we thank Dawn Marshall and Jacob Heiden for providing effective management of Safer-SIM project.

References

[1] *ABI research autonomous technologies*, https://www.abiresearch.com/press/abi-research-forecasts-8-million-vehicles-ship-sae-level-3-4-and-5-autonomous-technology-2025/, Accessed: 2010-09-30.

[2] J. J. Leonard, D. A. Mindell, and E. L. Stayton, *Autonomous vehicles, mobility, and employment policy: The roads ahead*, 2020.

[3] D. Elliott, W. Keen, and L. Miao, "Recent advances in connected and automated vehicles," *Journal of Traffic and Transportation Engineering (English Edition)*, vol. 6, no. 2, pp. 109–131, 2019.

[4] J. Sun, Z. Zheng, and J. Sun, "The relationship between car following string instability and traffic oscillations in finite-sized platoons and its use in easing congestion via connected and automated vehicles with idm based controller," *Transportation Research Part B: Methodological*, vol. 142, pp. 58–83, 2020.

[5] X. Li and A. J. Khattak, "Large-scale incident-induced congestion: En-route diversions of commercial and non-commercial traffic under connected and automated vehicles," in *2018 Winter Simulation Conference (WSC)*, IEEE, 2018, pp. 1132–1143.

[6] A. Nikitas, I. Kougias, E. Alyavina, and E. Njoya Tchouamou, "How can autonomous and connected vehicles, electromobility, brt, hyperloop, shared use mobility and mobility-as-a-service shape transport futures for the context of smart cities?" *Urban Science*, vol. 1, no. 4, p. 36, 2017.

[7] L. Yue, M. Abdel-Aty, Y. Wu, and L. Wang, "Assessment of the safety benefits of vehicles' advanced driver assistance, connectivity and low level automation systems," *Accident Analysis & Prevention*, vol. 117, pp. 55–64, 2018.

[8] M. S. Rahman, M. Abdel-Aty, J. Lee, and M. H. Rahman, "Safety benefits of arterials' crash risk under connected and automated vehicles," *Transportation Research Part C: Emerging Technologies*, vol. 100, pp. 354–371, 2019.

[9] D. J. Fagnant and K. Kockelman, "Preparing a nation for autonomous vehicles: Opportunities, barriers and policy recommendations," *Transportation Research Part A: Policy and Practice*, vol. 77, pp. 167–181, 2015.

[10] A. Papadoulis, M. Quddus, and M. Imprialou, "Estimating the corridor-level safety impact of connected and autonomous vehicles," Tech. Rep., 2018.

[11] J. SAE, "3016-2018, taxonomy and definitions for terms related to driving automation systems for on-road motor vehicles," *Society of Automobile Engineers, sae. org*, 2018.

[12] Y. Zheng, B. Ran, X. Qu, J. Zhang, and Y. Lin, "Cooperative lane changing strategies to improve traffic operation and safety nearby freeway off-ramps in a connected and automated vehicles environment," *IEEE Transactions on Intelligent Transportation Systems*, 2019.

[13] A. Papadoulis, M. Quddus, and M. Imprialou, "Evaluating the safety impact of connected and autonomous vehicles on motorways," *Accident Analysis & Prevention*, vol. 124, pp. 12–22, 2019.

[14] M. M. Morando, Q. Tian, L. T. Truong, and H. L. Vu, "Studying the safety impact of autonomous vehicles using simulation-based surrogate safety measures," *Journal of Advanced Transportation*, vol. 2018, 2018.

[15] M. Fyfe and T. Sayed, "Safety evaluation of connected vehicles for a cumulative travel time adaptive signal control microsimulation using the surrogate safety assessment model," Tech. Rep., 2017.

[16] J. Zhang, K. Wu, M. Cheng, M. Yang, Y. Cheng, and S. Li, "Safety evaluation for connected and autonomous vehicles' exclusive lanes considering penetrate ratios and impact of trucks using surrogate safety measures," *Journal of advanced transportation*, vol. 2020, 2020.

[17] N. Virdi, H. Grzybowska, S. T. Waller, and V. Dixit, "A safety assessment of mixed fleets with connected and autonomous vehicles using the surrogate safety assessment module," *Accident Analysis & Prevention*, vol. 131, pp. 95–111, 2019.

[18] M. Tajalli, M. Mehrabipour, and A. Hajbabaie, "Network-level coordinated speed optimization and traffic light control for connected and automated vehicles," *IEEE Transactions on Intelligent Transportation Systems*, 2020.

[19] M. Hasibur Rahman and M. Abdel-Aty, "Application of connected and automated vehicles in a large-scale network by considering vehicle-to-vehicle and vehicle-to-infrastructure technology," *Transportation Research Record*, p. 0 361 198 120 963 105, 2020.

[20] X. Wang, X. Wu, M. Abdel-Aty, and P. J. Tremont, "Investigation of road network features and safety performance," *Accident Analysis & Prevention*, vol. 56, pp. 22–31, 2013.

[21] J. Wang and H. Huang, "Road network safety evaluation using bayesian hierarchical joint model," *Accident Analysis & Prevention*, vol. 90, pp. 152–158, 2016.

[22] P. Xu, H. Huang, N. Dong, and S. Wong, "Revisiting crash spatial heterogeneity: A bayesian spatially varying coefficients approach," *Accident Analysis & Prevention*, vol. 98, pp. 330–337, 2017.

[23] M. Abdel-Aty, C. Siddiqui, H. Huang, and X. Wang, "Integrating trip and roadway characteristics to manage safety in traffic analysis zones," *Transportation Research Record*, vol. 2213, no. 1, pp. 20–28, 2011.

[24] C. Siddiqui and M. Abdel-Aty, "Nature of modeling boundary pedestrian crashes at zones," *Transportation research record*, vol. 2299, no. 1, pp. 31–40, 2012.

[25] J. Sun and J. Sun, "A dynamic bayesian network model for real-time crash prediction using traffic speed conditions data," *Transportation Research Part C: Emerging Technologies*, vol. 54, pp. 176–186, 2015.

[26] J. Ambros, V. Valentová, and J. Sedonık, "Developing updatable crash prediction model for network screening: Case study of czech two-lane rural road segments," *Transportation research record*, vol. 2583, no. 1, pp. 1–7, 2016.

[27] R. Bellman, "Dynamic programming," *Science*, vol. 153, no. 3731, pp. 34–37, 1966.

[28] R. S. Sutton and A. G. Barto, *Reinforcement learning: An introduction*. MIT press, 2018.

[29] D. P. Bertsekas and J. N. Tsitsiklis, "Neuro-dynamic programming: An overview," in *Proceedings of 1995 34th IEEE Conference on Decision and Control*, IEEE, vol. 1, 1995, pp. 560–564.

[30] W. B. Powell, *Approximate Dynamic Programming: Solving the curses of dimensionality*. John Wiley & Sons, 2007, vol. 703.

[31] J. H. Cho, H. S. Kim, and H. R. Choi, "An intermodal transport network planning algorithm using dynamic programming—a case study: From busan to rotterdam in intermodal freight routing," *Applied Intelligence*, vol. 36, no. 3, pp. 529–541, 2012.

[32] A. Medury and S. Madanat, "Incorporating network considerations into pavement management systems: A case for approximate dynamic programming," *Transportation Research Part C: Emerging Technologies*, vol. 33, pp. 134–150, 2013.

[33] C. Cai, C. K. Wong, and B. G. Heydecker, "Adaptive traffic signal control using approximate dynamic programming," *Transportation Research Part C: Emerging Technologies*, vol. 17, no. 5, pp. 456–474, 2009.

[34] J. Yin, T. Tang, L. Yang, Z. Gao, and B. Ran, "Energy-efficient metro train rescheduling with uncertain time-variant passenger demands: An approximate dynamic programming approach," *Transportation Research Part B: Methodological*, vol. 91, pp. 178–210, 2016.

[35] Y. Fan and Y. Nie, "Optimal routing for maximizing the travel time reliability," *Networks and Spatial Economics*, vol. 6, no. 3-4, pp. 333–344, 2006.

[36] Z. Qin, J. Tang, and J. Ye, "Deep reinforcement learning with applications in transportation," in *Proceedings of the 25th ACM SIGKDD International Conference on Knowledge Discovery & Data Mining*, 2019, pp. 3201–3202.

[37] I. Goodfellow, Y. Bengio, and A. Courville, *Deep learning*. MIT press, 2016.

[38] V. Mnih, K. Kavukcuoglu, D. Silver, A. Graves, I. Antonoglou, D. Wierstra, and M. Riedmiller, "Playing atari with deep reinforcement learning," *arXiv preprint arXiv:1312.5602*, 2013.

[39] D. Silver, A. Huang, C. J. Maddison, A. Guez, L. Sifre, G. Van Den Driessche, J. Schrittwieser, I. Antonoglou, V. Panneershelvam, M. Lanctot, *et al.*, "Mastering the game of go with deep neural networks and tree search," *nature*, vol. 529, no. 7587, p. 484, 2016.

[40] S. Gu, E. Holly, T. Lillicrap, and S. Levine, "Deep reinforcement learning for robotic manipulation with asynchronous off-policy updates," in *2017 IEEE international conference on robotics and automation (ICRA)*, IEEE, 2017, pp. 3389–3396.

[41] G. Zheng, F. Zhang, Z. Zheng, Y. Xiang, N. J. Yuan, X. Xie, and Z. Li, "Drn: A deep reinforcement learning framework for news recommendation," in *Proceedings of the 2018 World Wide Web Conference*, 2018, pp. 167–176.

[42] L. Li, Y. Lv, and F.-Y. Wang, "Traffic signal timing via deep reinforcement learning," *IEEE/CAA Journal of Automatica Sinica*, vol. 3, no. 3, pp. 247–254, 2016.

[43] C. Wu, A. Kreidieh, K. Parvate, E. Vinitsky, and A. M. Bayen, "Flow: Architecture and benchmarking for reinforcement learning in traffic control," *arXiv preprint arXiv:1710.05465*, 2017.

[44] K. Zhang, Z. Yang, and T. Başar, "Multi-agent reinforcement learning: A selective overview of theories and algorithms," *arXiv preprint arXiv:1911.10635*, 2019.

[45] H. S. Mahmassani, "Dynamic network traffic assignment and simulation methodology for advanced system management applications," *Networks and spatial economics*, vol. 1, no. 3-4, pp. 267–292, 2001.

[46] D.-Y. Lin, N. Eluru, S. T. Waller, and C. R. Bhat, "Integration of activity-based modeling and dynamic traffic assignment," *Transportation Research Record*, vol. 2076, no. 1, pp. 52–61, 2008.

[47] S. Sundaram, H. N. Koutsopoulos, M. Ben-Akiva, C. Antoniou, and R. Balakrishna, "Simulation-based dynamic traffic assignment for short-term planning applications," *Simulation Modelling Practice and Theory*, vol. 19, no. 1, pp. 450–462, 2011.

[48] C. Antoniou, H. N. Koutsopoulos, M. Ben-Akiva, and A. S. Chauhan, "Evaluation of diversion strategies using dynamic traffic assignment," *Transportation planning and technology*, vol. 34, no. 3, pp. 199–216, 2011.

[49] S. Gao, "Modeling strategic route choice and real-time information impacts in stochastic and time-dependent networks," *IEEE Transactions on Intelligent Transportation Systems*, vol. 13, no. 3, pp. 1298–1311, 2012.

[50] J. Ma, B. L. Smith, and X. Zhou, "Personalized real-time traffic information provision: Agent-based optimization model and solution framework," *Transportation Research Part C: Emerging Technologies*, vol. 64, pp. 164–182, 2016.

[51] M. Hasibur Rahman and M. Abdel-Aty, "Application of connected and automated vehicles in a large-scale network by considering vehicle-to-vehicle and vehicle-to-infrastructure technology," *Transportation Research Record: Journal of the Transportation Research Board*, vol. 2675, no. 1, 2021.

[52] T. Rambha, S. D. Boyles, A. Unnikrishnan, and P. Stone, "Marginal cost pricing for system optimal traffic assignment with recourse under supply-side uncertainty," *Transportation Research Part B: Methodological*, vol. 110, pp. 104–121, 2018.

[53] J. Wardrop, "Some theoretical aspects of road traffic research," *Proceedings of the Institute of Civil Engineers*, no. Part II, pp. 325–378, 1952.

[54] M. J. Beckmann, C. B. McGuire, and C. B. Winsten, "Studies in the economics of transportation," 1955.

[55] C. F. Daganzo and Y. Sheffi, "On stochastic models of traffic assignment," *Transportation science*, vol. 11, no. 3, pp. 253–274, 1977.

[56] H. Yang, "System optimum, stochastic user equilibrium, and optimal link tolls," *Transportation science*, vol. 33, no. 4, pp. 354–360, 1999.

[57] W. H.-K. Lam, Z. Gao, K. Chan, and H. Yang, "A stochastic user equilibrium assignment model for congested transit networks," *Transportation Research Part B: Methodological*, vol. 33, no. 5, pp. 351–368, 1999.

[58] M. G. Bell, "Stochastic user equilibrium assignment in networks with queues," *Transportation Research Part B: Methodological*, vol. 29, no. 2, pp. 125–137, 1995.

[59] D. K. Merchant and G. L. Nemhauser, "A model and an algorithm for the dynamic traffic assignment problems," *Transportation science*, vol. 12, no. 3, pp. 183–199, 1978.

[60] S. Peeta and A. K. Ziliaskopoulos, "Foundations of dynamic traffic assignment: The past, the present and the future," *Networks and spatial economics*, vol. 1, no. 3-4, pp. 233–265, 2001.

[61] Y.-C. Chiu, J. Bottom, M. Mahut, A. Paz, R. Balakrishna, T. Waller, and J. Hicks, "Dynamic traffic assignment: A primer," *Dynamic Traffic Assignment: A Primer*, 2011.

[62] T. L. Friesz and K. Han, "The mathematical foundations of dynamic user equilibrium," *Transportation research part B: methodological*, vol. 126, pp. 309–328, 2019.

[63] F. He, Y. Yin, and S. Lawphongpanich, "Network equilibrium models with battery electric vehicles," *Transportation Research Part B: Methodological*, vol. 67, pp. 306–319, 2014.

[64] T.-G. Wang, C. Xie, J. Xie, and T. Waller, "Path-constrained traffic assignment: A trip chain analysis under range anxiety," *Transportation Research Part C: Emerging Technologies*, vol. 68, pp. 447–461, 2016.

[65] H. Zheng, X. He, Y. Li, and S. Peeta, "Traffic equilibrium and charging facility locations for electric vehicles," *Networks and Spatial Economics*, vol. 17, no. 2, pp. 435–457, 2017.

[66] X. Di and X. J. Ban, "A unified equilibrium framework of new shared mobility systems," *Transportation Research Part B: Methodological*, vol. 129, pp. 50–78, 2019.

[67] J. Wang, S. Peeta, and X. He, "Multiclass traffic assignment model for mixed traffic flow of human-driven vehicles and connected and autonomous vehicles," *Transportation Research Part B: Methodological*, vol. 126, pp. 139–168, 2019.

[68] L. Du, L. Han, and X.-Y. Li, "Distributed coordinated in-vehicle online routing using mixed-strategy congestion game," *Transportation Research Part B: Methodological*, vol. 67, pp. 1–17, 2014.

[69] L. Du, L. Han, and S. Chen, "Coordinated online in-vehicle routing balancing user optimality and system optimality through information perturbation," *Transportation Research Part B: Methodological*, vol. 79, pp. 121–133, 2015.

[70] A. Unnikrishnan and S. T. Waller, "User equilibrium with recourse," *Networks and Spatial Economics*, vol. 9, no. 4, p. 575, 2009.

[71] S. D. Boyles and S. T. Waller, “A mean-variance model for the minimum cost flow problem with stochastic arc costs,” *Networks*, vol. 56, no. 3, pp. 215–227, 2010.

[72] D. Calderone and S. S. Sastry, “Markov decision process routing games,” in *2017 ACM/IEEE 8th International Conference on Cyber-Physical Systems (ICCPS)*, IEEE, 2017, pp. 273–280.

[73] R. J.-B. Wets, “Chapter viii stochastic programming,” *Handbooks in operations research and management science*, vol. 1, pp. 573–629, 1989.

[74] M. Beckmann, C. McGuire, and C. B. Winsten, “Studies in the economics of transportation,” Tech. Rep., 1956.

[75] Y. Sheffi, *Urban transportation networks*. Prentice-Hall, Englewood Cliffs, NJ, 1985, vol. 6.

[76] D. Branston, “Link capacity functions: A review,” *Transportation research*, vol. 10, no. 4, pp. 223–236, 1976.

[77] L. Pu, R. Joshi, S. Energy, *et al.*, “Surrogate safety assessment model (ssam)–software user manual,” Turner-Fairbank Highway Research Center, Tech. Rep., 2008.

[78] G. Klunder, A. Abdoelbasier, and B. Immers, “Development of a micro-simulation model to predict road traffic safety on intersections with surrogate safety measures,” *, 1-8*, 2006.

[79] D. V. Killi and P. Vedagiri, “Proactive evaluation of traffic safety at an unsignalized intersection using micro-simulation,” *Journal of Traffic and Logistics Engineering Vol*, vol. 2, no. 2, 2014.

[80] O. Giuffrè, A. Granà, M. L. Tumminello, T. Giuffrè, S. Trubia, A. Sferlazza, and M. Rencelj, “Evaluation of roundabout safety performance through surrogate safety measures from microsimulation,” *Journal of Advanced Transportation*, vol. 2018, 2018.

[81] A. Stevanovic, J. Stevanovic, and C. Kergaye, “Optimization of traffic signal timings based on surrogate measures of safety,” *Transportation research part C: emerging technologies*, vol. 32, pp. 159–178, 2013.

[82] Z. Li, S. Ahn, K. Chung, D. R. Ragland, W. Wang, and J. W. Yu, "Surrogate safety measure for evaluating rear-end collision risk related to kinematic waves near freeway recurrent bottlenecks," *Accident Analysis & Prevention*, vol. 64, pp. 52–61, 2014.

[83] P. Zhao and C. Lee, "Assessing rear-end collision risk of cars and heavy vehicles on freeways using a surrogate safety measure," *Accident Analysis & Prevention*, vol. 113, pp. 149–158, 2018.

[84] M. M. Minderhoud and P. H. Bovy, "Extended time-to-collision measures for road traffic safety assessment," *Accident Analysis & Prevention*, vol. 33, no. 1, pp. 89–97, 2001.

[85] K. Ozbay, H. Yang, B. Bartin, and S. Mudigonda, "Derivation and validation of new simulation-based surrogate safety measure," *Transportation research record*, vol. 2083, no. 1, pp. 105–113, 2008.

[86] V. Astarita, G. Guido, A. Vitale, and V. Giofré, "A new microsimulation model for the evaluation of traffic safety performances," 2012.

[87] M. Okamura, A. Fukuda, H. Morita, H. Suzuki, and M. Nakazawa, "Impact evaluation of a driving support system on traffic flow by microscopic traffic simulation," *Advances in Transportation Studies*, no. Special Issue 2011, 2011.

[88] S. Almqvist, C. Hydén, and R. Risser, "Use of speed limiters in cars for increased safety and a better environment," *Transportation Research Record*, no. 1318, 1991.

[89] F. J. C. Cunto and F. F. Saccomanno, "Microlevel traffic simulation method for assessing crash potential at intersections," Tech. Rep., 2007.

[90] O. Bagdadi and A. Várhelyi, "Jerky driving—an indicator of accident proneness?" *Accident Analysis & Prevention*, vol. 43, no. 4, pp. 1359–1363, 2011.

[91] C. Hydén, "Traffic conflicts technique: State-of-the-art," *Traffic safety work with video processing*, vol. 37, pp. 3–14, 1996.

[92] P. G. Michael, F. C. Leeming, and W. O. Dwyer, "Headway on urban streets: Observational data and an intervention to decrease tailgating," *Transportation research part F: traffic psychology and behaviour*, vol. 3, no. 2, pp. 55–64, 2000.

[93] C. Hydén, "The development of a method for traffic safety evaluation: The swedish traffic conflicts technique," *Bulletin Lund Institute of Technology, Department*, no. 70, 1987.

[94] A. Svensson, *A method for analysing the traffic process in a safety perspective*. Lund Institute of Technology Sweden, 1998.

[95] B. L. Allen, B. T. Shin, and P. J. Cooper, "Analysis of traffic conflicts and collisions," Tech. Rep., 1978.

[96] P. Songchitruksa and A. P. Tarko, "Practical method for estimating frequency of right-angle collisions at traffic signals," *Transportation research record*, vol. 1953, no. 1, pp. 89–97, 2006.

[97] J. Hou, G. F. List, and X. Guo, "New algorithms for computing the time-to-collision in freeway traffic simulation models," *Computational intelligence and neuroscience*, vol. 2014, 2014.

[98] Y. Kuang, X. Qu, and Y. Yan, "Will higher traffic flow lead to more traffic conflicts? a crash surrogate metric based analysis," *PLoS one*, vol. 12, no. 8, e0182458, 2017.

[99] R. Alsalhi, V. V. Dixit, and V. V. Gayah, "On the existence of network macroscopic safety diagrams: Theory, simulation and empirical evidence," *PloS one*, vol. 13, no. 8, e0200541, 2018.

[100] S. S. Mahmud, L. Ferreira, M. S. Hoque, and A. Tavassoli, "Application of proximal surrogate indicators for safety evaluation: A review of recent developments and research needs," *IATSS research*, vol. 41, no. 4, pp. 153–163, 2017.

[101] J. Hogema and W. Janssen, "Effects of intelligent cruise control on driving behaviour: A simulator study," TNO, Tech. Rep., 1996.

[102] A. R. A. Van der Horst, "A time-based analysis of road user behaviour in normal and critical encounters.," 1991.

[103] K. Vogel, "A comparison of headway and time to collision as safety indicators," *Accident analysis & prevention*, vol. 35, no. 3, pp. 427–433, 2003.

[104] T. Sayed, M. H. Zaki, and J. Autey, "Automated safety diagnosis of vehicle–bicycle interactions using computer vision analysis," *Safety science*, vol. 59, pp. 163–172, 2013.

[105] F. Huang, P. Liu, H. Yu, and W. Wang, “Identifying if vissim simulation model and ssam provide reasonable estimates for field measured traffic conflicts at signalized intersections,” *Accident Analysis & Prevention*, vol. 50, pp. 1014–1024, 2013.

[106] S. Hirst, “Of collision warnings,” *Ergonomics and Safety of Intelligent Driver Interfaces; Loughborough University: Loughborough, UK*, p. 203, 1997.

[107] Q. Shi and M. Abdel-Aty, “Big data applications in real-time traffic operation and safety monitoring and improvement on urban expressways,” *Transportation Research Part C: Emerging Technologies*, vol. 58, pp. 380–394, 2015.

Appendix A

Figures of Four-Node Test Network

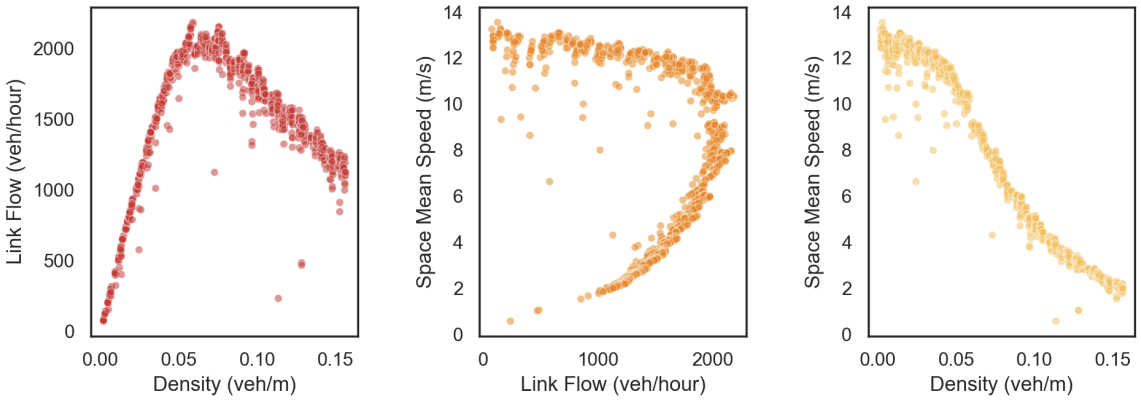

Figure A.1: Fundamental Diagram of Link e1

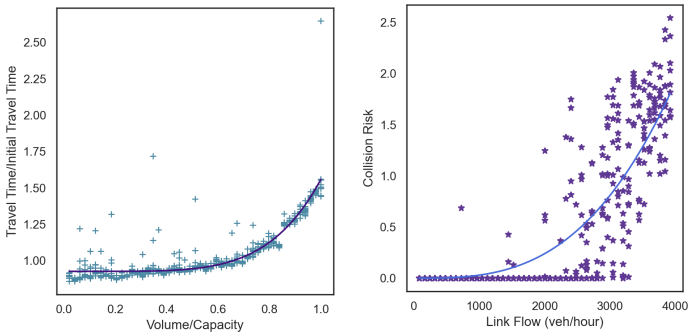

Figure A.2: Link Performance Function and Relation between Collision Risk and Link Flow for Link e1

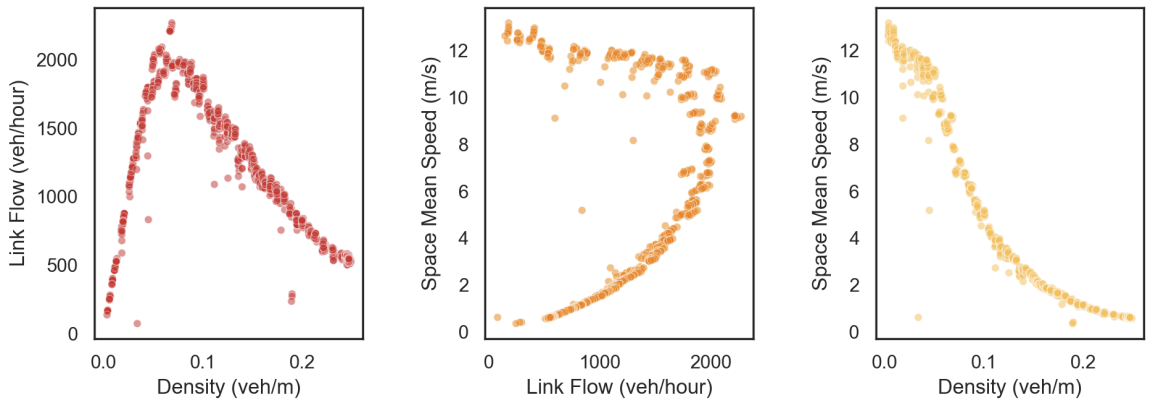

Figure A.3: Fundamental Diagram of Link e2

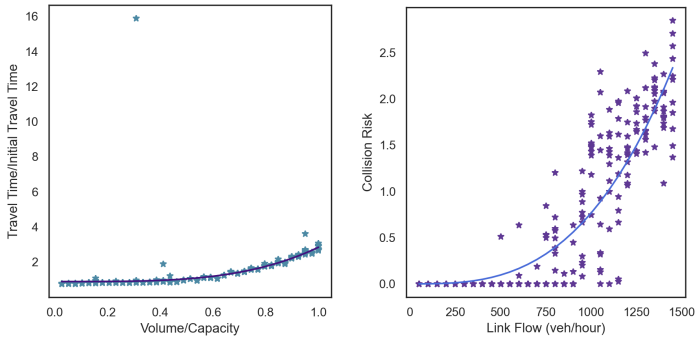

Figure A.4: Link Performance Function and Relation between Collision Risk and Link Flow for Link e2

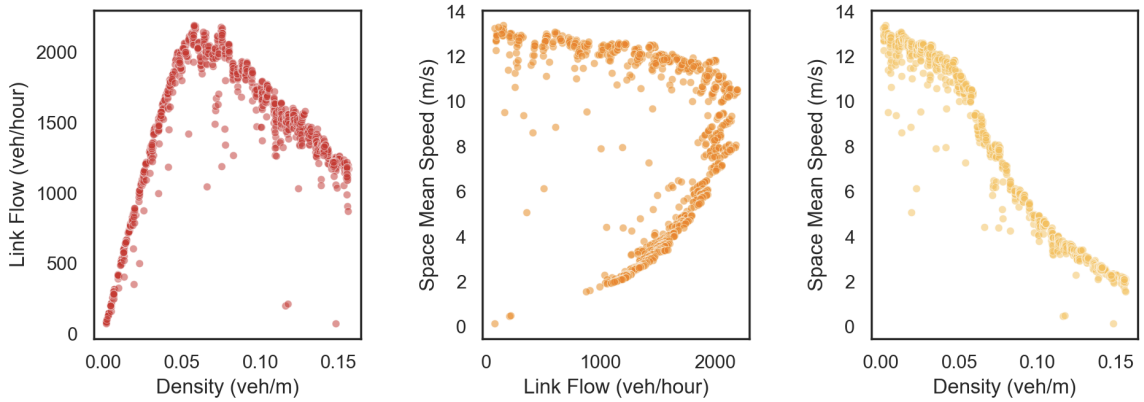

Figure A.5: Fundamental Diagram of Link e4

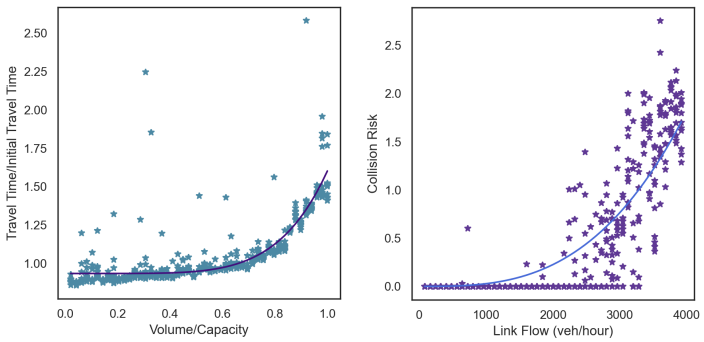

Figure A.6: Link Performance Function and Relation between Collision Risk and Link Flow for Link e4

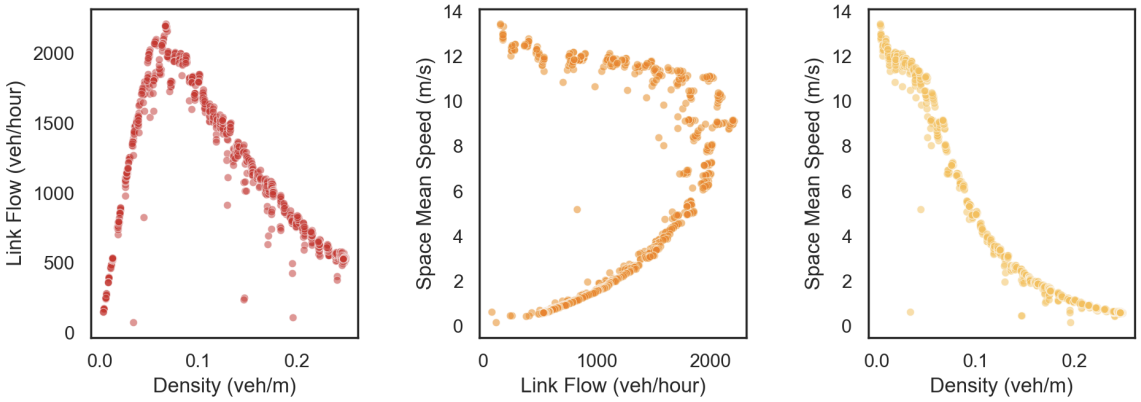

Figure A.7: Fundamental Diagram of Link e5

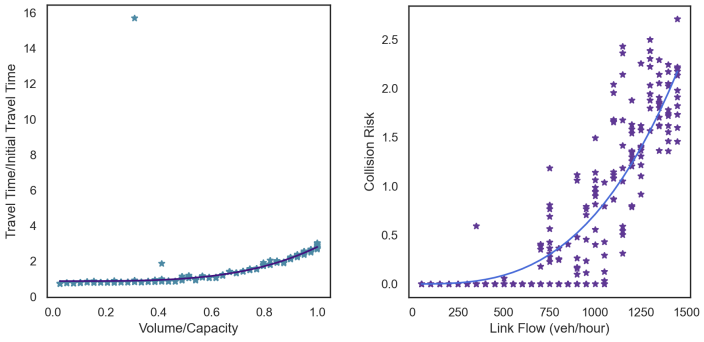

Figure A.8: Link Performance Function and Relation between Collision Risk and Link Flow for Link e5

Appendix B

Equations of Four-Node Test Network

Link e1

$$CR = 0.0022 + 1.068e-6 \times (LinkFlow) + 1.134e-10 \times (LinkFlow)^2$$

$$t = 141.05 + 0.767(\frac{v_a}{C_a})^{3.946}$$

Link e2

$$CR = 0.0029 + 4.398e-6 \times (LinkFlow) + 4.862e-10 \times (LinkFlow)^2$$

$$t = 162.95 + 2.821(\frac{v_a}{C_a})^{3.586}$$

Link e3

$$CR = 0.0032 + 3.61e-6 \times (LinkFlow) + 8.417e-10 \times (LinkFlow)^2$$

$$t = 146.843 + 2.701(\frac{v_a}{C_a})^{3.411}$$

Link e4

$$CR = 0.0031 + 7.706e-8 \times (LinkFlow) + 2.939e-10 \times (LinkFlow)^2$$

$$t = 140.988 + 0.782(\frac{v_a}{C_a})^{4.173}$$

Link e5

$$CR = 0.0034 + 4.016e-6 \times (LinkFlow) + 6.773e-10 \times (LinkFlow)^2$$

$$t = 165.079 + 2.301(\frac{v_a}{C_a})^{3.672}$$

Appendix C

Orlando Network Results

Link 1-2 and 2-1

$$t = 120 + 0.15(\frac{v_a}{9200})^4$$

$$CR\,(p_i) \;=\; \frac{e^{-5.8835 \,+\, X_i \;\; 0.0007}}{1 \;+\; e^{-5.8835 \,+\, X_i \;\; 0.0007}}$$

Link 2-4 and 4-2

$$t = 60 + 0.15(\frac{v_a}{4400})^4$$

$$CR\,(p_i) \;=\; \frac{e^{-8.4944 \,+\, X_i \;\; 0.0014}}{1 \;+\; e^{-8.4944 \,+\, X_i \;\; 0.0014}}$$

Link 1-3 and 3-1

$$t = 60 + 0.15(\frac{v_a}{9200})^4$$

$$CR\ (p_i)\ =\ \frac{e^{-5.8791\ +\ X_i\ \ 0.0005}}{1\ +\ e^{-5.8791\ +\ X_i\ \ 0.0005}}$$

Link 3-4 and 4-3

$$t = 120 + 0.15(\frac{v_a}{6600})^4$$

$$CR\ (p_i)\ =\ \frac{e^{-7.6803\ +\ X_i\ \ 0.0029}}{1\ +\ e^{-7.6803\ +\ X_i\ \ 0.0029}}$$

Link 3-5 and 5-3

$$t = 360 + 0.15(\frac{v_a}{9200})^4$$

$$CR\ (p_i)\ =\ \frac{e^{-4.2791\ +\ X_i\ \ 0.0003}}{1\ +\ e^{-4.2791\ +\ X_i\ \ 0.0003}}$$

Link 5-10 and 10-5

$$t = 180 + 0.15(\frac{v_a}{9600})^4$$

$$CR\ (p_i)\ =\ \frac{e^{-5.1920\ +\ X_i\ \ 0.0006}}{1\ +\ e^{-5.1920\ +\ X_i\ \ 0.0006}}$$

Link 5-11 and 11-5

$$t = 180 + 0.15(\frac{v_a}{9200})^4$$

$$CR\ (p_i)\ =\ \frac{e^{-4.6374\ +\ X_i\ \ 0.0004}}{1\ +\ e^{-4.6374\ +\ X_i\ \ 0.0004}}$$

Link 11-12 and 12-11

$$t = 60 + 0.15(\frac{v_a}{8800})^4$$

$$CR\ (p_i)\ =\ \frac{e^{-5.8288\ +\ X_i\ \ 0.0003}}{1\ +\ e^{-5.8288\ +\ X_i\ \ 0.0003}}$$

Link 12-13 and 13-12

$$t = 120 + 0.15(\frac{v_a}{8400})^4$$

$$CR\ (p_i)\ =\ \frac{e^{-5.2844\ +\ X_i\ \ 0.0004}}{1\ +\ e^{-5.2844\ +\ X_i\ \ 0.0004}}$$

Link 13-10 and 10-13

$$t = 180 + 0.15(\frac{v_a}{9600})^4$$

$$CR\ (p_i)\ =\ \frac{e^{-4.7818\ +\ X_i\ \ 0.0002}}{1\ +\ e^{-4.7818\ +\ X_i\ \ 0.0002}}$$

Link 13-14 and 14-13

$$t = 120 + 0.15(\frac{v_a}{8400})^4$$

$$CR\ (p_i)\ =\ \frac{e^{-5.6073\ +\ X_i\ \ 0.0003}}{1\ +\ e^{-5.6073\ +\ X_i\ \ 0.0003}}$$

Link 10-14 and 14-10

$$t = 60 + 0.15(\frac{v_a}{9600})^4$$

$$CR\ (p_i)\ =\ \frac{e^{-6.1302\ +\ X_i\ \ 0.0079}}{1\ +\ e^{-6.1302\ +\ X_i\ \ 0.0079}}$$

Link 4-6 and 6-4

$$t = 300 + 0.15(\frac{v_a}{4600})^4$$

$$CR\ (p_i)\ =\ \frac{e^{-5.8051\ +\ X_i\ \ 0.0011}}{1\ +\ e^{-5.8051\ +\ X_i\ \ 0.0011}}$$

Link 4-7 and 7-4

$$t = 480 + 0.15(\frac{v_a}{4400})^4$$

$$CR\ (p_i)\ =\ \frac{e^{-10.9543\ +\ X_i\ \ 0.000006}}{1\ +\ e^{-10.9543\ +\ X_i\ \ 0.000006}}$$

Link 6-7 and 7-6

$$t = 180 + 0.15(\frac{v_a}{7200})^4$$

$$CR\ (p_i)\ =\ \frac{e^{-10.9543\ +\ X_i\ \ 0.000006}}{1\ +\ e^{-10.9543\ +\ X_i\ \ 0.000006}}$$

Link 6-10 and 10-6

$$t = 240 + 0.15(\frac{v_a}{7200})^4$$

$$CR\left(p_i\right) = \frac{e^{-10.9543 + X_i \quad 0.000006}}{1 + e^{-10.9543 + X_i \quad 0.000006}}$$

Link 6-9 and 9-6

$$t = 60 + 0.15(\frac{v_a}{4800})^4$$

$$CR\left(p_i\right) = \frac{e^{-10.9543 + X_i \quad 0.000006}}{1 + e^{-10.9543 + X_i \quad 0.000006}}$$

Link 7-8 and 8-7

$$t = 120 + 0.15(\frac{v_a}{4400})^4$$

$$CR\left(p_i\right) = \frac{e^{-10.9543 + X_i \quad 0.000006}}{1 + e^{-10.9543 + X_i \quad 0.000006}}$$

Link 9-8 and 8-9

$$t = 240 + 0.15(\frac{v_a}{6000})^4$$

$$CR\left(p_i\right) = \frac{e^{-10.9543 + X_i \quad 0.000006}}{1 + e^{-10.9543 + X_i \quad 0.000006}}$$

Link 9-14 and 14-9

$$t = 480 + 0.15(\frac{v_a}{6000})^4$$

$$CR\left(p_i\right) = \frac{e^{-4.7099 + X_i \quad 0.0014}}{1 + e^{-4.7099 + X_i \quad 0.0014}}$$

Link 8-16 and 16-8

$$t = 180 + 0.15(\frac{v_a}{4400})^4$$

$$CR\ (p_i)\ =\ \frac{e^{-4.4609\ +\ X_i\ \ 0.0006}}{1\ +\ e^{-4.4609\ +\ X_i\ \ 0.0006}}$$

Link 9-15 and 15-9

$$t = 60 + 0.15(\frac{v_a}{6000})^4$$

$$CR\ (p_i)\ =\ \frac{e^{-6.4915\ +\ X_i\ \ -0.0001}}{1\ +\ e^{-6.4915\ +\ X_i\ \ -0.0001}}$$

Link 15-16 and 16-15

$$t = 120 + 0.15(\frac{v_a}{6000})^4$$

$$CR\ (p_i)\ =\ \frac{e^{-5.3167\ +\ X_i\ \ 0.0006}}{1\ +\ e^{-5.3167\ +\ X_i\ \ 0.0006}}$$

Link 14-15 and 15-14

$$t = 240 + 0.15(\frac{v_a}{7200})^4$$

$$CR\ (p_i)\ =\ \frac{e^{-4.4551\ +\ X_i\ \ 0.0006}}{1\ +\ e^{-4.4551\ +\ X_i\ \ 0.0006}}$$

Link 14-17 and 17-14

$$t = 360 + 0.15(\frac{v_a}{9000})^4$$

$$CR\ (p_i)\ =\ \frac{e^{-3.9633\ +\ X_i\ \ 0.0012}}{1\ +\ e^{-3.9633\ +\ X_i\ \ 0.0012}}$$

Link 15-18 and 18-15

$$t = 240 + 0.15(\frac{v_a}{4800})^4$$

$$CR\ (p_i)\ =\ \frac{e^{-10.9543\ +\ X_i\ \ 0.000006}}{1\ +\ e^{-10.9543\ +\ X_i\ \ 0.000006}}$$

Link 17-18 and 18-17

$$t = 420 + 0.15(\frac{v_a}{5000})^4$$

$$CR\ (p_i)\ =\ \frac{e^{-10.9543\ +\ X_i\ \ 0.000006}}{1\ +\ e^{-10.9543\ +\ X_i\ \ 0.000006}}$$

Table C.1: All the Possible Routes for 6 OD Flow

Route	Links
0	[(3, 1), (1, 2), (2, 4), (4, 6), (6, 10), (10, 5), (5, 11)]
1	[(3, 4), (4, 6), (6, 10), (10, 5), (5, 11)]
2	[(3, 4), (4, 6), (6, 10), (10, 13), (13, 12), (12, 11)]
3	[(3, 4), (4, 6), (6, 10), (10, 14), (14, 13), (13, 12), (12, 11)]
4	[(3, 4), (4, 6), (6, 9), (9, 14), (14, 10), (10, 5), (5, 11)]
5	[(3, 4), (4, 6), (6, 9), (9, 14), (14, 13), (13, 12), (12, 11)]
6	[(3, 4), (4, 7), (7, 6), (6, 10), (10, 5), (5, 11)]
7	[(3, 4), (4, 7), (7, 6), (6, 10), (10, 13), (13, 12), (12, 11)]
8	[(3, 5), (5, 11)]
9	[(3, 5), (5, 10), (10, 13), (13, 12), (12, 11)]
10	[(3, 5), (5, 10), (10, 14), (14, 13), (13, 12), (12, 11)]
11	[(3, 1), (1, 2), (2, 4), (4, 6), (6, 10), (10, 14), (14, 17)]
12	[(3, 1), (1, 2), (2, 4), (4, 6), (6, 9), (9, 14), (14, 17)]
13	[(3, 4), (4, 6), (6, 10), (10, 13), (13, 14), (14, 17)]
14	[(3, 4), (4, 6), (6, 10), (10, 14), (14, 15), (15, 18), (18, 17)]
15	[(3, 4), (4, 6), (6, 10), (10, 14), (14, 17)]
16	[(3, 4), (4, 6), (6, 7), (7, 8), (8, 9), (9, 14), (14, 17)]
17	[(3, 4), (4, 6), (6, 9), (9, 14), (14, 15), (15, 18), (18, 17)]
18	[(3, 4), (4, 6), (6, 9), (9, 14), (14, 17)]
19	[(3, 4), (4, 6), (6, 9), (9, 15), (15, 14), (14, 17)]
20	[(3, 4), (4, 6), (6, 9), (9, 15), (15, 18), (18, 17)]
21	[(3, 4), (4, 7), (7, 6), (6, 10), (10, 13), (13, 14), (14, 17)]
22	[(3, 4), (4, 7), (7, 6), (6, 10), (10, 14), (14, 17)]
23	[(3, 4), (4, 7), (7, 6), (6, 9), (9, 14), (14, 17)]
24	[(3, 4), (4, 7), (7, 6), (6, 9), (9, 15), (15, 14), (14, 17)]
25	[(3, 4), (4, 7), (7, 6), (6, 9), (9, 15), (15, 18), (18, 17)]
26	[(3, 4), (4, 7), (7, 8), (8, 9), (9, 14), (14, 17)]
27	[(3, 4), (4, 7), (7, 8), (8, 9), (9, 15), (15, 14), (14, 17)]
28	[(3, 4), (4, 7), (7, 8), (8, 9), (9, 15), (15, 18), (18, 17)]
29	[(3, 4), (4, 7), (7, 8), (8, 16), (16, 15), (15, 14), (14, 17)]
30	[(3, 4), (4, 7), (7, 8), (8, 16), (16, 15), (15, 18), (18, 17)]

Route	Links
31	[(3, 5), (5, 11), (11, 12), (12, 13), (13, 10), (10, 14), (14, 17)]
32	[(3, 5), (5, 11), (11, 12), (12, 13), (13, 14), (14, 17)]
33	[(3, 5), (5, 10), (10, 6), (6, 9), (9, 14), (14, 17)]
34	[(3, 5), (5, 10), (10, 6), (6, 9), (9, 15), (15, 14), (14, 17)]
35	[(3, 5), (5, 10), (10, 6), (6, 9), (9, 15), (15, 18), (18, 17)]
36	[(3, 5), (5, 10), (10, 13), (13, 14), (14, 15), (15, 18), (18, 17)]
37	[(3, 5), (5, 10), (10, 13), (13, 14), (14, 17)]
38	[(3, 5), (5, 10), (10, 14), (14, 9), (9, 15), (15, 18), (18, 17)]
39	[(3, 5), (5, 10), (10, 14), (14, 15), (15, 18), (18, 17)]
40	[(3, 5), (5, 10), (10, 14), (14, 17)]
41	[(11, 5), (5, 3)]
42	[(11, 5), (5, 10), (10, 6), (6, 4), (4, 2), (2, 1), (1, 3)]
43	[(11, 5), (5, 10), (10, 6), (6, 4), (4, 3)]
44	[(11, 5), (5, 10), (10, 6), (6, 7), (7, 4), (4, 3)]
45	[(11, 5), (5, 10), (10, 14), (14, 9), (9, 6), (6, 4), (4, 3)]
46	[(11, 12), (12, 13), (13, 10), (10, 5), (5, 3)]
47	[(11, 12), (12, 13), (13, 10), (10, 6), (6, 4), (4, 3)]
48	[(11, 12), (12, 13), (13, 10), (10, 6), (6, 7), (7, 4), (4, 3)]
49	[(11, 12), (12, 13), (13, 14), (14, 9), (9, 6), (6, 4), (4, 3)]
50	[(11, 12), (12, 13), (13, 14), (14, 10), (10, 5), (5, 3)]
51	[(11, 12), (12, 13), (13, 14), (14, 10), (10, 6), (6, 4), (4, 3)]
52	[(11, 5), (5, 3), (3, 4), (4, 6), (6, 10), (10, 14), (14, 17)]
53	[(11, 5), (5, 3), (3, 4), (4, 6), (6, 9), (9, 14), (14, 17)]
54	[(11, 5), (5, 10), (10, 6), (6, 9), (9, 14), (14, 17)]
55	[(11, 5), (5, 10), (10, 6), (6, 9), (9, 15), (15, 14), (14, 17)]
56	[(11, 5), (5, 10), (10, 6), (6, 9), (9, 15), (15, 18), (18, 17)]
57	[(11, 5), (5, 10), (10, 13), (13, 14), (14, 15), (15, 18), (18, 17)]
58	[(11, 5), (5, 10), (10, 13), (13, 14), (14, 17)]
59	[(11, 5), (5, 10), (10, 14), (14, 9), (9, 15), (15, 18), (18, 17)]
60	[(11, 5), (5, 10), (10, 14), (14, 15), (15, 18), (18, 17)]
61	[(11, 5), (5, 10), (10, 14), (14, 17)]

Route	Links
62	[(11, 12), (12, 13), (13, 10), (10, 6), (6, 9), (9, 14), (14, 17)]
63	[(11, 12), (12, 13), (13, 10), (10, 14), (14, 15), (15, 18), (18, 17)]
64	[(11, 12), (12, 13), (13, 10), (10, 14), (14, 17)]
65	[(11, 12), (12, 13), (13, 14), (14, 9), (9, 15), (15, 18), (18, 17)]
66	[(11, 12), (12, 13), (13, 14), (14, 15), (15, 18), (18, 17)]
67	[(11, 12), (12, 13), (13, 14), (14, 17)]
	, (4, 2), (2, 1), (1, 3)]
	(4, 3)]
70	[(17, 14), (14, 9), (9, 6), (6, 10), (10, 5), (5, 3)]
71	[(17, 14), (14, 9), (9, 6), (6, 7), (7, 4), (4, 3)]
72	[(17, 14), (14, 9), (9, 8), (8, 7), (7, 4), (4, 3)]
73	[(17, 14), (14, 9), (9, 8), (8, 7), (7, 6), (6, 4), (4, 3)]
74	[(17, 14), (14, 10), (10, 5), (5, 3)]
75	[(17, 14), (14, 10), (10, 6), (6, 4), (4, 2), (2, 1), (1, 3)]
76	[(17, 14), (14, 10), (10, 6), (6, 4), (4, 3)]
77	[(17, 14), (14, 10), (10, 6), (6, 7), (7, 4), (4, 3)]
78	[(17, 14), (14, 10), (10, 13), (13, 12), (12, 11), (11, 5), (5, 3)]
79	[(17, 14), (14, 13), (13, 10), (10, 5), (5, 3)]
80	[(17, 14), (14, 13), (13, 10), (10, 6), (6, 4), (4, 3)]
81	[(17, 14), (14, 13), (13, 10), (10, 6), (6, 7), (7, 4), (4, 3)]
82	[(17, 14), (14, 13), (13, 12), (12, 11), (11, 5), (5, 3)]
83	[(17, 14), (14, 15), (15, 9), (9, 6), (6, 4), (4, 3)]
84	[(17, 14), (14, 15), (15, 9), (9, 6), (6, 10), (10, 5), (5, 3)]
85	[(17, 14), (14, 15), (15, 9), (9, 6), (6, 7), (7, 4), (4, 3)]
86	[(17, 14), (14, 15), (15, 9), (9, 8), (8, 7), (7, 4), (4, 3)]
87	[(17, 14), (14, 15), (15, 16), (16, 8), (8, 7), (7, 4), (4, 3)]
88	[(17, 18), (18, 15), (15, 9), (9, 6), (6, 4), (4, 3)]
89	[(17, 18), (18, 15), (15, 9), (9, 6), (6, 10), (10, 5), (5, 3)]
90	[(17, 18), (18, 15), (15, 9), (9, 6), (6, 7), (7, 4), (4, 3)]
91	[(17, 18), (18, 15), (15, 9), (9, 8), (8, 7), (7, 4), (4, 3)]
92	[(17, 18), (18, 15), (15, 9), (9, 14), (14, 10), (10, 5), (5, 3)]

Route	Links
93	[(17, 18), (18, 15), (15, 14), (14, 9), (9, 6), (6, 4), (4, 3)]
94	[(17, 18), (18, 15), (15, 14), (14, 10), (10, 5), (5, 3)]
95	[(17, 18), (18, 15), (15, 14), (14, 10), (10, 6), (6, 4), (4, 3)]
96	[(17, 18), (18, 15), (15, 14), (14, 13), (13, 10), (10, 5), (5, 3)]
97	[(17, 18), (18, 15), (15, 16), (16, 8), (8, 7), (7, 4), (4, 3)]
98	[(17, 14), (14, 9), (9, 6), (6, 4), (4, 3), (3, 5), (5, 11)]
99	[(17, 14), (14, 9), (9, 6), (6, 10), (10, 5), (5, 11)]
100	[(17, 14), (14, 9), (9, 6), (6, 10), (10, 13), (13, 12), (12, 11)]
101	[(17, 14), (14, 10), (10, 5), (5, 11)]
102	[(17, 14), (14, 10), (10, 6), (6, 4), (4, 3), (3, 5), (5, 11)]
103	[(17, 14), (14, 10), (10, 13), (13, 12), (12, 11)]
104	[(17, 14), (14, 13), (13, 10), (10, 5), (5, 11)]
105	[(17, 14), (14, 13), (13, 12), (12, 11)]
106	[(17, 14), (14, 15), (15, 9), (9, 6), (6, 10), (10, 5), (5, 11)]
107	[(17, 18), (18, 15), (15, 9), (9, 6), (6, 10), (10, 5), (5, 11)]
108	[(17, 18), (18, 15), (15, 9), (9, 14), (14, 10), (10, 5), (5, 11)]
109	[(17, 18), (18, 15), (15, 9), (9, 14), (14, 13), (13, 12), (12, 11)]
110	[(17, 18), (18, 15), (15, 14), (14, 10), (10, 5), (5, 11)]
111	[(17, 18), (18, 15), (15, 14), (14, 10), (10, 13), (13, 12), (12, 11)]
112	[(17, 18), (18, 15), (15, 14), (14, 13), (13, 10), (10, 5), (5, 11)]
113	[(17, 18), (18, 15), (15, 14), (14, 13), (13, 12), (12, 11)]